

IC/76/79



793/79
v.2

IC/76/79
INTERNAL REPORT
(Limited distribution)

0 000 000 023188 M

International Atomic Energy Agency

and

United Nations Educational Scientific and Cultural Organization

INTERNATIONAL CENTRE FOR THEORETICAL PHYSICS

T O P I C A L M E E T I N G

ON LEPTON INTERACTIONS AND NEW PARTICLES

6 - 9 July 1976

P A R T I I

(Contributions)

MIRAMARE - TRIESTE

July 1976

e^+e^- PHYSICS AT DESY

G.W. Buschhorn

Max-Planck Institut für Physik und Astrophysik, Föhringer Ring 6,
8 München, Fed. Rep. Germany.

DESY 76/37
July 1976

by

W. Braunschweig, H.-U. Martyn, H.G. Sander, D. Schmitz, W. Sturm, and W. Waltraff,
I. Physikalisches Institut der RWTH Aachen

D. Cords, R. Feist, R. Fries, E. Gadermann, B. Gittelmann, H. Hulschig, P. Joos,
W. Koch, U. Kötze, H. Kreibiel, D. Kreinick, W.A. McNeely, K.C. Moffeit,
P. Petersen, O. Römer, R. Rüsck, B.H. Wijk, and G. Wolf
Deutsches Elektronen-Synchrotron DESY, Hamburg

G. Grindhammer, J. Ludwig, K.H. Mess, G. Poelz, J. Ringel, K. Sauerberg, and
P. Schmüser,

II. Institut für Experimentalphysik der Universität Hamburg

W. DeBoer, G. Buschhorn, B. Gunderson, R. Kotthaus, H. Lierl, H. Oberlack, and
M. Schliwa

Max-Planck-Institut für Physik und Astrophysik, München

S. Orito, T. Suda, Y. Totsuka, and S. Yamada
University of Tokyo, Tokyo

Abstract:

Single electrons produced with hadrons in e^+e^- collisions at cms energies of 4.0 to 4.2 GeV have been observed at DORIS using the double arm spectrometer DASP. The measured electron spectrum peaks at low momentum and the associated hadron multiplicity is high. These experimental results are consistent with the electromagnetic production and weak decay of a hadron with a new quantum number that is conserved by the strong and electromagnetic interaction. The electron yield at 3.7 GeV (the ψ' resonance) and at lower energies was found to be consistent with the estimated background, indicating that the production threshold lies between 3.7 and 4.0 GeV.

Using the double arm spectrometer, DASP, a search for final states containing an electron and hadrons has been made at the e^+e^- colliding ring DORIS. Mixed electron-hadron final states might arise from the production and decay of a pair of heavy leptons, $L\bar{L}$ ⁽¹⁾. The observed final state would be created by the leptonic decay of one particle ($L \rightarrow \nu_L \nu_e$) and the semi leptonic decay of the other ($L \rightarrow \nu_L + \text{hadrons}$). An alternative source of electron-hadron final states is the production of a new hadron, H , that is inhibited from decaying strongly or electromagnetically. Such a hadron would have to possess a new quantum number ⁽²⁾. To conserve this quantum number in the electromagnetic production process the H particles must be produced in pairs. The observed electron would come from either the weak leptonic decay $H \rightarrow e + \nu_e$ or the semi leptonic decay $H \rightarrow e + \nu_e + \text{hadrons}$.

The DASP detector consists of two identical magnetic spectrometer arms symmetrical with respect to the interaction point. Both arms together cover a geometrical solid angle of 0.9 sr. A large aperture non-magnetic detector is mounted between the magnets. A detailed description of this set up can be found elsewhere ⁽³⁾. For the present measurements the electron identification was improved by installing threshold Cerenkov counters on each side of the beam tube (see figure 1). The counters, which covered the geometric acceptance of the magnets, were filled with Freon 114 ($n = 1.0014$) at atmospheric pressure. Data were collected at cms energies between 4.0 and 4.2 GeV for a total integrated luminosity of 670 nb⁻¹. The detector was triggered on a single charged particle traversing a spectrometer arm, firing the scintillation counters, S_0 and S_M , mounted before the magnet, and one of the time of flight counters and a shower counter located at the rear. For most of the experiment, the magnet was powered at 1/3 full excitation corresponding to a cut off momentum of 0.2 GeV/c.

Events with electrons were selected by requiring a signal in the appropriate Cerenkov counter. 4500 events were found. 1900 events have only a single electron with no additional track in the inner detector. A preliminary analysis ⁽⁴⁾ showed that these events come from the reaction $e^+e^- \rightarrow e^+e^-\gamma$ where one of the electrons and the photon escape down the beam tube. Since these events are copious and easily recognized, they have been used to study the detector response to low momentum electrons.

Events coming from pure electromagnetic interactions such as,

$$\begin{aligned} e^+ e^- &\rightarrow e^+ e^- \\ e e &\rightarrow e e \\ &+ e^+ e^- \\ &+ e e \gamma \\ &+ e^+ e^- + e^+ e^- \\ &+ e e e e \end{aligned}$$

were removed by requiring at least one non-showering charged particle track in the inner detector. A showering particle may be separated from a non-showering one by counting the number of proportional tubes that have fired in the vicinity of its track. A non-showering track was defined as one in which the particle traversed at least 5 of 9 tube layers along its path and on the average activated less than 1.5 tubes per layer. In a sample of π^0 events, 85 % of the charged pion tracks were correctly identified as non-showering and more than 90 % of the photons of energy greater than 200 MeV were labeled showering by this criterion. The recognition of a showering particle improves with energy. For example the above criterion correctly identifies 1.5 GeV Bhabha electrons 97.5 % of the time.

After requiring a non-showering track in the inner detector, the sample of potential electron-hadron events was reduced to 87. The following background processes were considered as sources of the residual events: -

1. Dalitz decays of π^0 (η^0) or pair conversion of photons in the material in front of the Cerenkov counter.
2. Misidentification of hadrons as electrons in the Cerenkov counter.
3. Inelastic electron scattering from the gas in the storage ring.
4. Compton scattering in the material in front of the Cerenkov counter.
5. Decays of pions and kaons into electrons.
6. $e^+ + e^- \rightarrow e^+ + e^- + e^-$ + hadrons from two photon exchange.
7. Cascade decay through an intermediate state with a large branching ratio into $e^+ e^-$ pairs.

Dalitz decays and pair conversions can be excluded by using pulse height information from S_0 and S_M . The correlated pulse height of S_0 vs S_M for the remaining 87 events is shown in figure 2a. A distinct clustering of events is seen at $S_0 = 110$, $S_M = 110$ corresponding to a minimum ionizing particle. A cut was

imposed as shown by the dotted line. When this cut was applied to the control sample of events having only a single electron, 20 % of them were rejected. This cut was also found to be helpful in eliminating beam gas events.

Pions passing through the Cerenkov counter occasionally produce an energetic δ ray, which fires the counter. However, the pulse height in the shower counters behind the magnet provides an independent means of identifying electrons. In figure 2b, the shower counter pulse height versus the particle momentum is shown for the 47 surviving events. The solid lines indicate the region for 90 % electron acceptance, as determined from the sample of events having only a single electron. Most of the events lie within the area defined by these lines. Events with momenta greater than 200 MeV/c and shower pulse height greater than 125 were accepted as indicated by the dotted lines.

The distribution of vertex position along the beam axis is shown in figure 2c for the remaining 34 events. Events produced by beam gas scattering should uniformly populate the region within 10 cm of the center of the interaction diamond. We cut on vertex position as shown in the figure. After the cut, 28 events remain with an estimated background of 0.9 events.

Compton back scattering of a photon from an electron in the material in front of the Cerenkov counter could masquerade as an electron-hadron final state if the electron recoiled into the outer detector. However in this case only electrons and no positrons would be observed. Among the remaining events, 17 have positrons and 11 have electrons.

The semi leptonic decay of neutral and charged kaons is another potential source of background. For the process $K^+ \rightarrow e^+ X$ to contribute, the kaon must decay before reaching the middle of the Cerenkov counter. For the K^0 to contribute, it must decay before the S_0 counter. Using the number of charged kaons observed in these data runs we expect less than 1 background event from this source.

The production of electron hadron final states from the 2 photon mechanism was calculated for the DASP detector (5). Less than 1 event is expected. Furthermore, the angular distribution from the 2γ process is sharply peaked forward, changing by several orders of magnitude over the range of the spectrometer acceptance. In figure 3, the angular distribution of the remaining events is plotted. The distribution is flat with no apparent forward peaking.

Still another possible source of electron hadron events is the cascade decay through an intermediate state which has a large branching ratio into electron pairs. Both the ψ and ψ' are good candidates for such a state, e.g.

$$e^+ e^- \rightarrow j/\psi + \pi^+ \pi^- + e^+ + e^- + \pi^0$$

However, such events would be recognized because they contain a second electron. Of the 28 remaining events only a few have an additional showering charged track and some of these could be pions. Furthermore, the electrons from j/ψ and ψ' decay are energetic (one electron has an energy greater than 1.55 GeV and the other, greater than 1 GeV). The observed electrons all have momenta below 900 MeV/c. The observed electron momentum distribution would be consistent with the decay of a slowly moving particle of mass ~ 600 MeV into $e^+ e^-$. The only known candidates in this mass region are the ω^0 and ϕ^0 , and their branching ratio is more than 2 orders of magnitude too small.

To check the above background estimates and to demonstrate the existence of a threshold energy, data were collected at the ψ' resonance (54 nb^{-1}) and at cms energies of 3.60, 3.62, and 3.68 GeV (266 nb^{-1}). At the ψ' resonance 1.1 times as many inclusive hadron events were recorded as in the data taken above 4 GeV. An analysis similar to the one just described yielded 9 events. Four of these were identified as cascade decays through the $\psi(3.1)$ resonance. The remainder of 5 events is consistent with our expectation for the background. We conclude that the electron signal observed at higher energies is not due to misidentification of ordinary multihadron events. Three events were found in the data below the ψ' resonance. If the yield above 4 GeV came from an electromagnetic process, one would have expected 13 events here.

After all cuts, 28 events remain with an electron and at least one non-showering particle track. Conventional sources could produce ~ 7 events. We believe the non-showering tracks to be hadrons because almost all of the charged tracks in the events with high multiplicity are non-showering. Aside from high order electromagnetic processes, of which the 2γ process is the most likely to provide a significant contribution, electron-hadron final states are produced only by the weak interaction. Therefore we conclude that we have observed the production of a new particle which can only decay via the weak interaction.

It is not possible to account for all the events as coming from the production of heavy sequential lepton pairs. Following models for the decay modes of a heavy lepton⁽⁶⁾, we calculate an average of 3 or fewer tracks from charged particles or gamma rays per detected event. Most events should have only one electron and

a charged pion. In fig. 4 the spectrum of the number of detected particle tracks is plotted. Only 6 of the 28 events above 4 GeV have an observed multiplicity of two or three. In the "background" data 2 of the 5 events at the ψ' and 2 of the 3 events below ψ' had this low multiplicity. In the remaining discussion only the 22 events of multiplicity 4 or more are used.

Additional evidence comes from the electron momentum spectrum. For heavy sequential lepton production the observed electron comes from the leptonic decay. If one assumes a value for the associated neutrino mass, the momentum spectrum of the electron can be calculated. The acceptance corrected momentum spectrum of the 22 high multiplicity events is plotted in figure 5. The dotted curve is the expected distribution for V-A theory, a massless neutrino, and a heavy lepton mass of 1.9 GeV. (V + A theory gives a similar distribution.) The curve is inconsistent with the data. If the curve is normalized to fit the data below 700 MeV/c, it predicts 28 observed events above 700 MeV/c. In principle one could fit the momentum spectrum by assuming a neutrino mass of about 1 GeV, but this is difficult to reconcile with the observed high multiplicity. Both the momentum spectrum and the observed multiplicity indicate that the events do not come from heavy sequential lepton production⁽⁷⁾.

A new meson with only weak decays may yield any of the following states

- (a) $H \rightarrow e^+ e^-$ or $\mu^+ \mu^-$
- (b) $H \rightarrow e^+ e^- + \text{hadrons}$ or $\mu^+ \mu^- + \text{hadrons}$
- (c) $H \rightarrow \text{hadrons}$

Decay mode a) would lead to high momentum electrons. Since none are seen, we assume this mode is suppressed (for example by helicity conservation). If decay mode b) is the source of the electrons that we observe, the associated hadrons will lead to lower electron momenta than those calculated for the leptonic decay of the heavy lepton. A relatively high hadron multiplicity for H decays is expected, primarily because both semileptonic and purely hadronic decay modes are available. Also additional hadrons might be created in the production process. Low electron momenta and high multiplicities are in fact observed. Therefore, the most likely interpretation of the data is that the bulk of the events come from the semileptonic decay of a hadron with a new quantum number that is respected by the strong and electromagnetic interaction. The mass of the new hadron lies between 1.8 and 2.1 GeV.

On the basis of the angular distribution shown in figure 3 we assume that the electrons are isotropic and calculate a lower limit for the production cross section times branching ratio into electrons.

$$\sigma(e^+e^- \rightarrow e + \text{hadrons}) \approx 2 B(H \rightarrow e\bar{e}) \sigma(e^+e^- \rightarrow H\bar{H}) > 1 \text{ nb}$$

This implies a substantial production cross section between 4 GeV and 4.2 GeV in the center of mass.

The observed properties of these events are compatible with the predictions of the Charm model (2). However, it remains to be shown that the weak current responsible for these events couples preferentially to strange mesons.

Acknowledgements

We are indebted to Dr. Degèle and the DORIS machine group for their inventiveness and diligence which made this experiment possible. We thank Drs. John Ellis, K. Fujikawa, I. Karliner, C. Llewellyn-Smith and T. Walsh for many discussions. The invaluable cooperation with the technical support groups and the computer center at DESY is gratefully acknowledged. We thank all the engineers and technicians of the collaborating institutions of DASP. B. Gittelman wishes to thank the Alexander von Humboldt Foundation for the grant which enabled him to spend this year at the DESY Laboratory. The non-DESY members of the collaboration thank the DESY Direktorium for the kind hospitality extended to them.

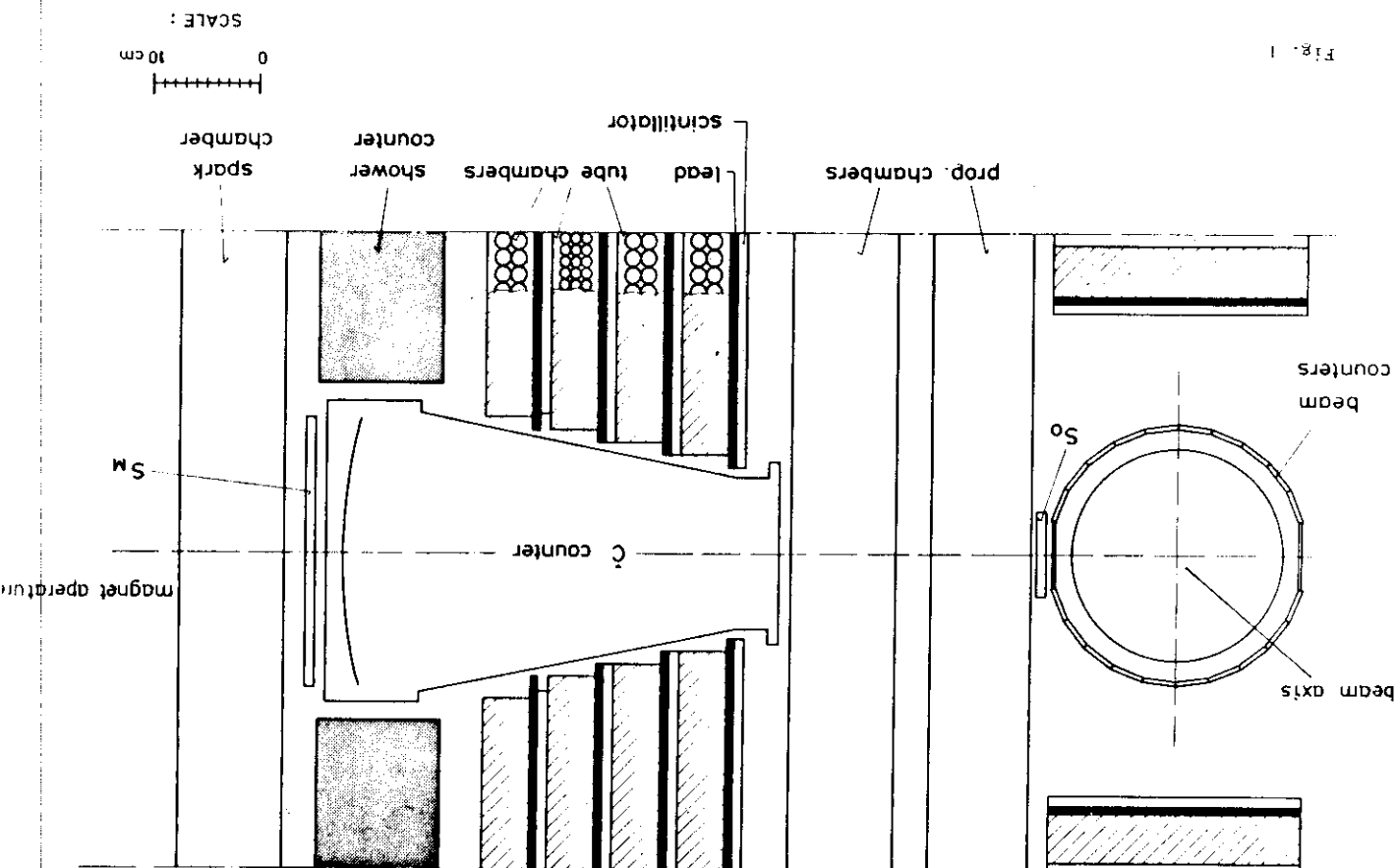
References

- 1) Evidence for a new heavy lepton has been published:
M. Perl et al., Phys. Rev. Letters 35, 1489 (1975).
M. Perl, Invited Talk at the 1976 Neutrino Conference, Aachen.
- 2) Charm is an example of such a new quantum number.
Y. Hara, Phys. Rev. 134B, 701 (1964).
J.D. Bjorken and S.L. Glashow, Phys. Lett. 11, 255 (1964).
S.L. Glashow, J. Illiopoulos and L. Maiani, Phys. Rev. D2, 1285 (1970).
Evidence for a new hadron of mass 1865 ± 15 MeV, with properties indicative of its possessing charm, has been reported.
G. Goldhaber et al., SLAC-PUB-1762, LBL 5309, June 1976. (Submitted to Phys. Rev. Letters).
- 3) DASP collaboration, Phys. Letters 53B, 393 (1974).
DASP collaboration, Phys. Letters 57B, 297 (1975).
DASP collaboration, Phys. Letters 57B, 407 (1975).
- 4) We wish to thank F.A. Berend for the evaluation of the cross section.
- 5) T. Walsh, private communication.
- 6) The final states expected in the decay of a sequential heavy lepton have been evaluated by several authors
Y.S. Tsai, Phys. Rev. D4, 2821 (1971).
J.D. Bjorken and C.H. Llewellyn-Smith, Phys. Rev. D7, 887 (1973).
K. Fujikawa and N. Kawamoto, DESY Preprint 76/01.
K.J.F. Gaemers and R. Raito, SLAC-PUB-1727 (1976).
- 7) Other lepton hypotheses such as a heavy electron with a large branching ratio into electron plus hadrons are not excluded by the above arguments.

Figure Captions

1. A section of the DASP inner detector showing the counter and spark chamber arrangement on one side of the interaction point. The Cerenkov counter is located in front of the magnet aperture of the outer spectrometer.
2. Data distributions at various steps in the event purification procedure.
 - a. Pulse height distribution in the scintillation counters before and after the Cerenkov counter.
 - b. Shower counter pulse height vs momentum of the electron in the outer detector.
 - c. Distribution of the event vertex along the beam axis. Arrows indicate the region of acceptable events.
3. The production angular distribution of the electrons in the outer detector. The abscissa defines the cosine of the production angle with respect to the initial electron of the same sign charge (ie. forward and backward production angles are distinguished).
4. Observed number of tracks per event. Since an electron plus one non-showering charged track was required, the smallest track count is 2.
5. Acceptance corrected electron momentum distribution for events with 4 or more tracks. The curve was calculated for the leptonic decay of a particle of mass 1.9 GeV and normalized to fit the observed events between 200 and 700 MeV/c.

Fig. 1



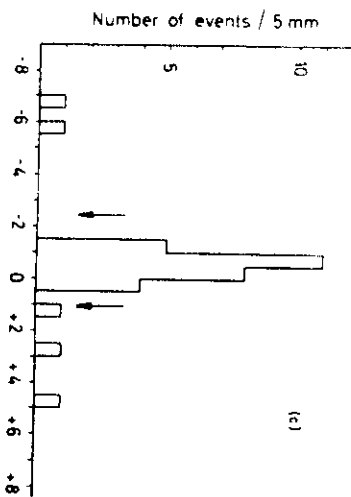
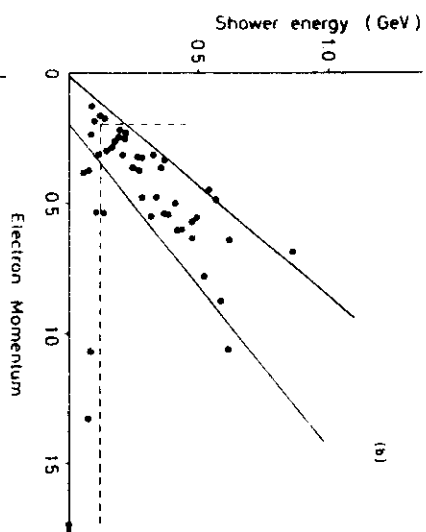
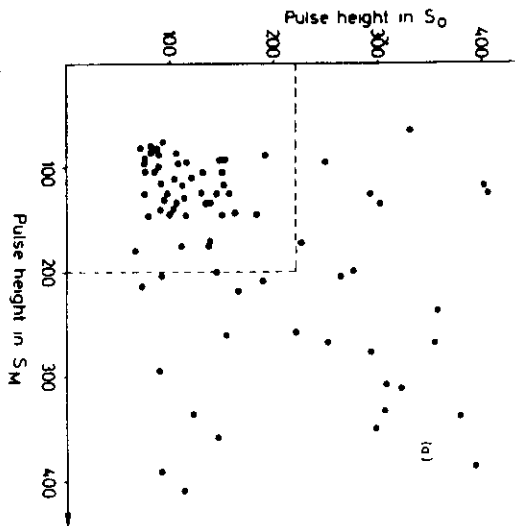


Fig. 2 vertex position, Z (cm)

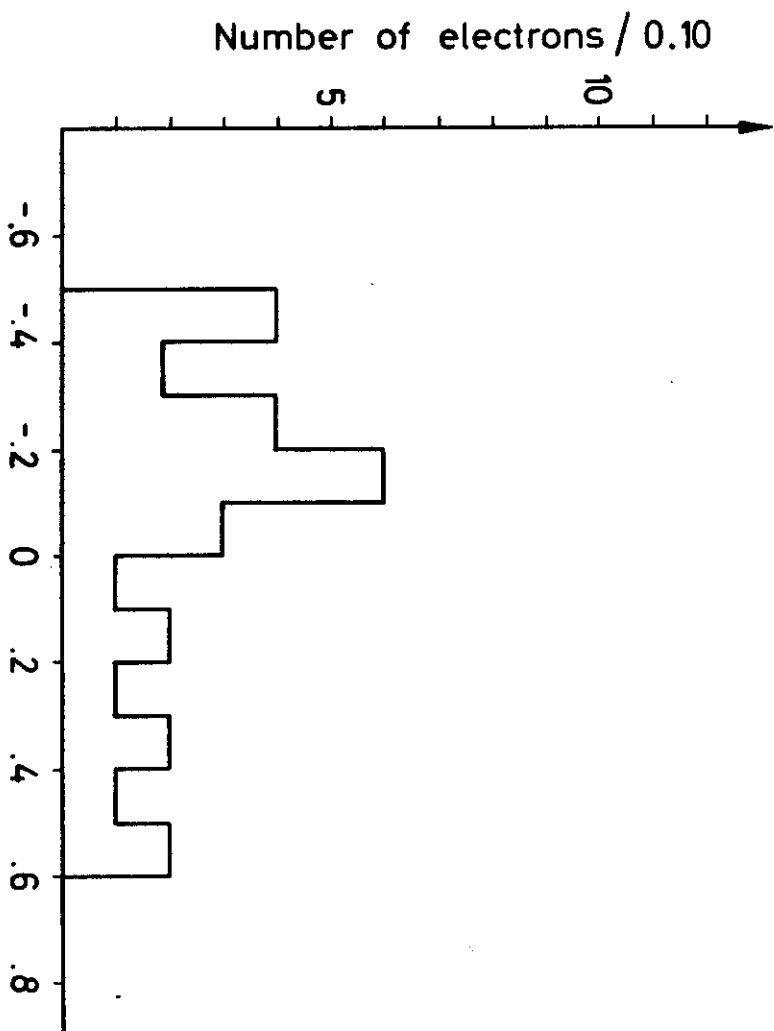


Fig. 3

Fig. 4

Sum of charged and neutral tracks

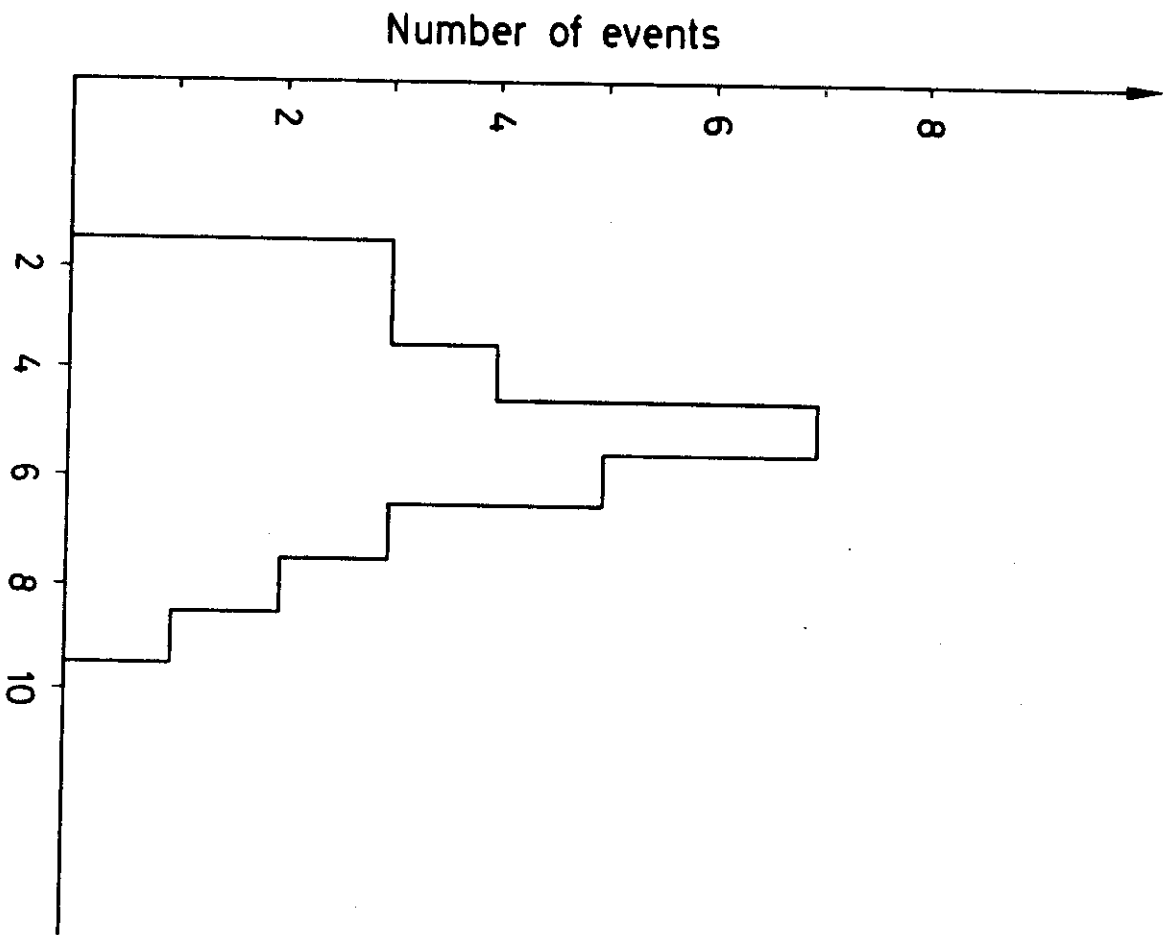
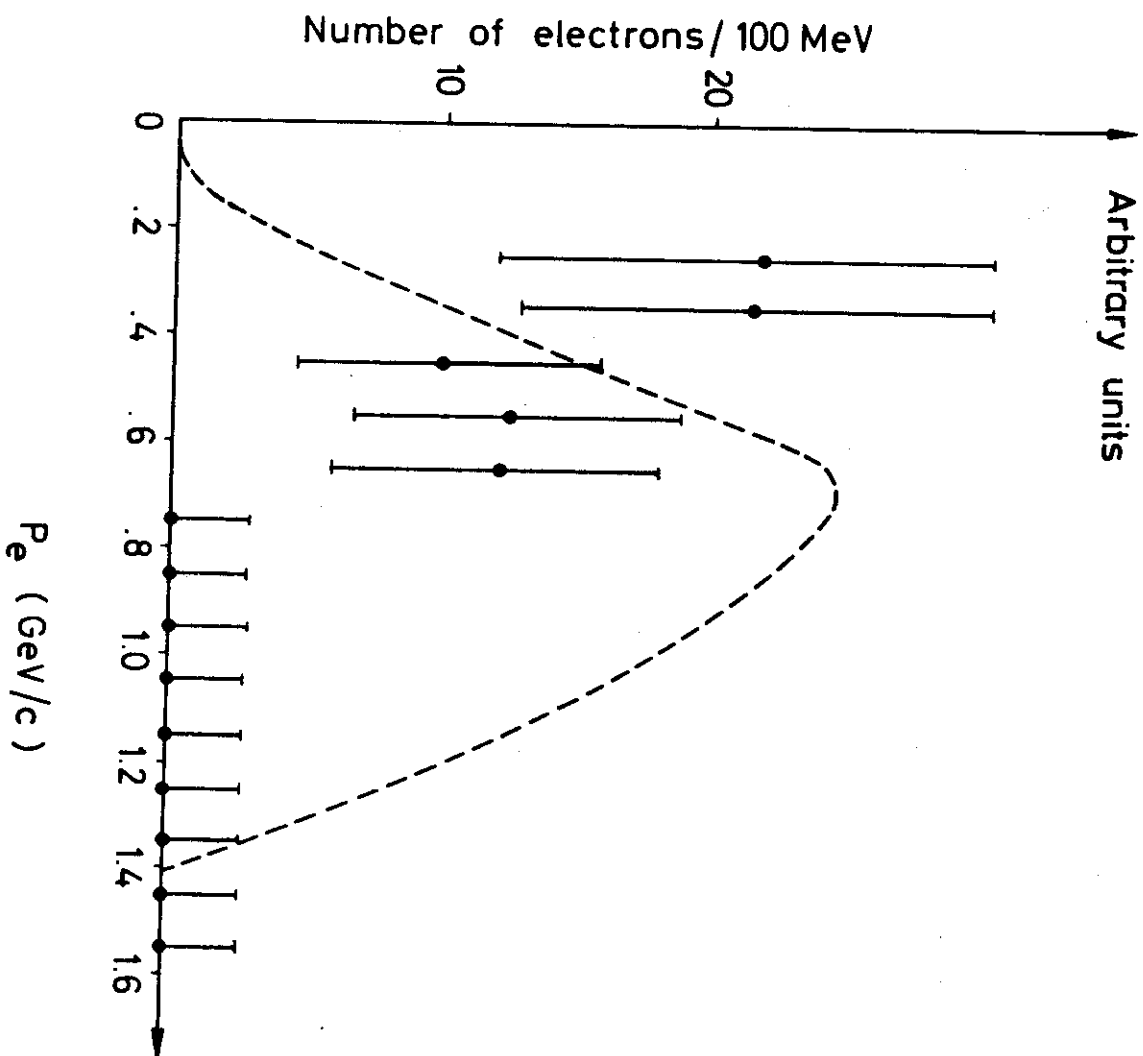


Fig. 5



Recent results from VORIS

G. Buschhorn, Max Planck Inst. Munich

Data from 3 collaborations:

DASP: Aachen - DESY + Hamburg -
Munich MPI - Tokio

PLUTO: DESY + Hamburg - Siegen -
Wuppertal

Neutr. Det.: DESY - Heidelberg

I New results on the decay of J/ψ and ψ'

1. - status of X
2. - $P_c(X)$
3. - J/ψ -decay modes

II Recent results on the 4.0 - 4.3 GeV region

~~to be added~~

- leptons (e) from weak decays
of hadrons \approx DESY 76/37 (DASP)
(results from Pluto as H. Meyer)

I.1 Status of $X(2800)$ (DASP)

Stanford Conf. 1975 :

preliminary data from DASP-
and DESY-Heidelberg - Coll. on

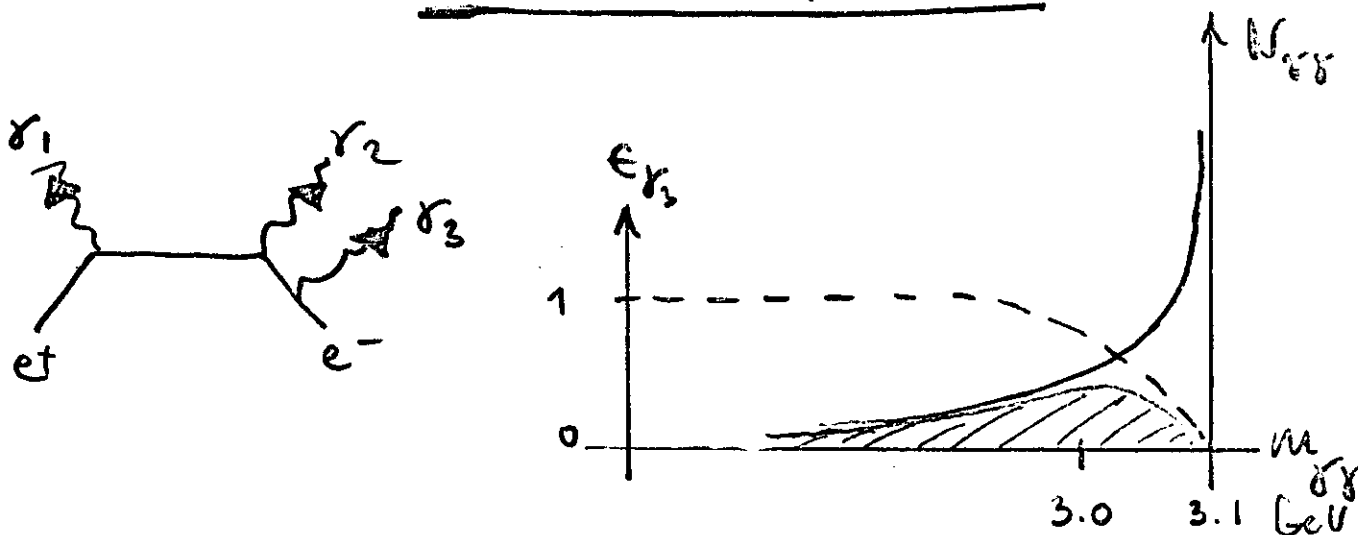
$$J/\psi \rightarrow \gamma + (X \rightarrow 2\gamma)$$

$$m_X \simeq 2.8 \text{ GeV}$$

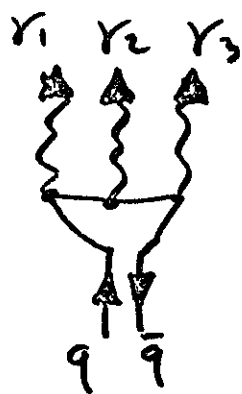
$X \equiv$ paracharm. ground state $1'S_0 (" \chi_c)?$

Now about double statistics

Problem : QED - background



direct decay $J/\psi \rightarrow 3\gamma$



Pelaquier-Renard
 - $\Gamma(J/\psi \rightarrow 3\gamma) \approx \text{few eV}$
 - no peaks in $m_{\gamma\gamma}$

DASP

fig. 1

inner detector ^{fig. 2} ($\Omega \approx 0.7 \cdot 4\pi$)
 consisting of

4 * (scint. hod. | 5mm Pb | 3(2) prop. tube layer)
 + shower counter (BX₀ Pb-scint.)

from test runs :

" γ " : ≥ 2 prop. tubes + follow. scint.

ϵ_γ : $\approx 96\%$ for $E_\gamma \geq 200$ MeV
 ($\approx 50\%$ at 60 MeV)

$\Delta\theta_\gamma$: $\pm 2^\circ$

(45)

DASP-Collaboration

W. Braunschweig, H.-U. Martyn, H.G. Sander, D. Schmitz, W. Sturm, W. Wallraff,
I. Physikalisches Institut der RWTH Aachen,

K. Berkelman², D. Cords, R. Felst, E. Gadermann, B. Gittelman⁺, H. Hultschig,
P. Joos, W. Koch, U. Kötz, H. Krehbiel, D. Kreinick, W.A. McNeely, K.C. Moffeit,
A. Petersen, B.H. Wiik, and G. Wolf,
Deutsches Elektronen-Synchrotron DESY

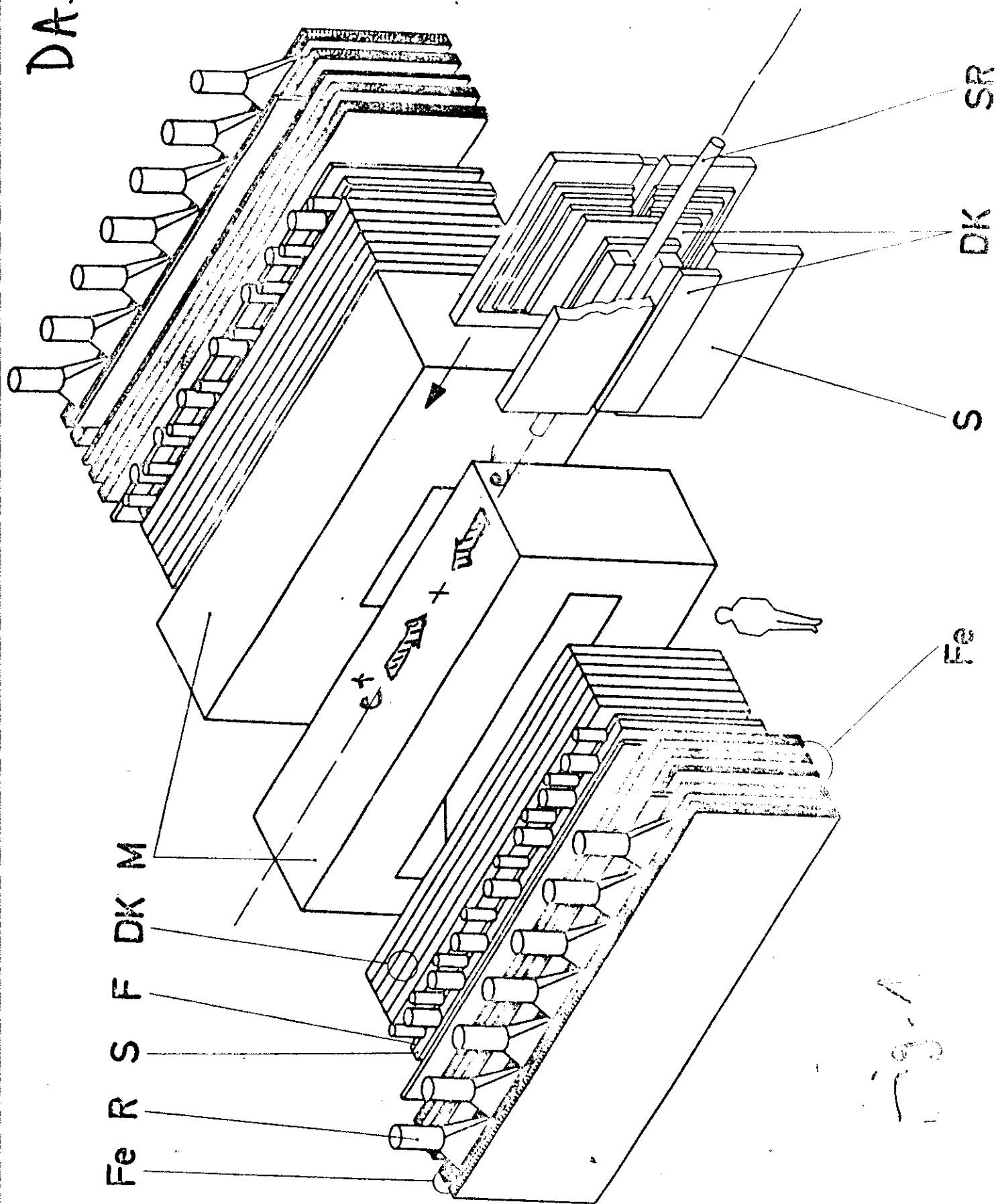
G. Grindhammer, J. Ludwig, K.-H. Mess, G. Poelz, J. Ringel, K. Sauerberg,
P. Schmüser,

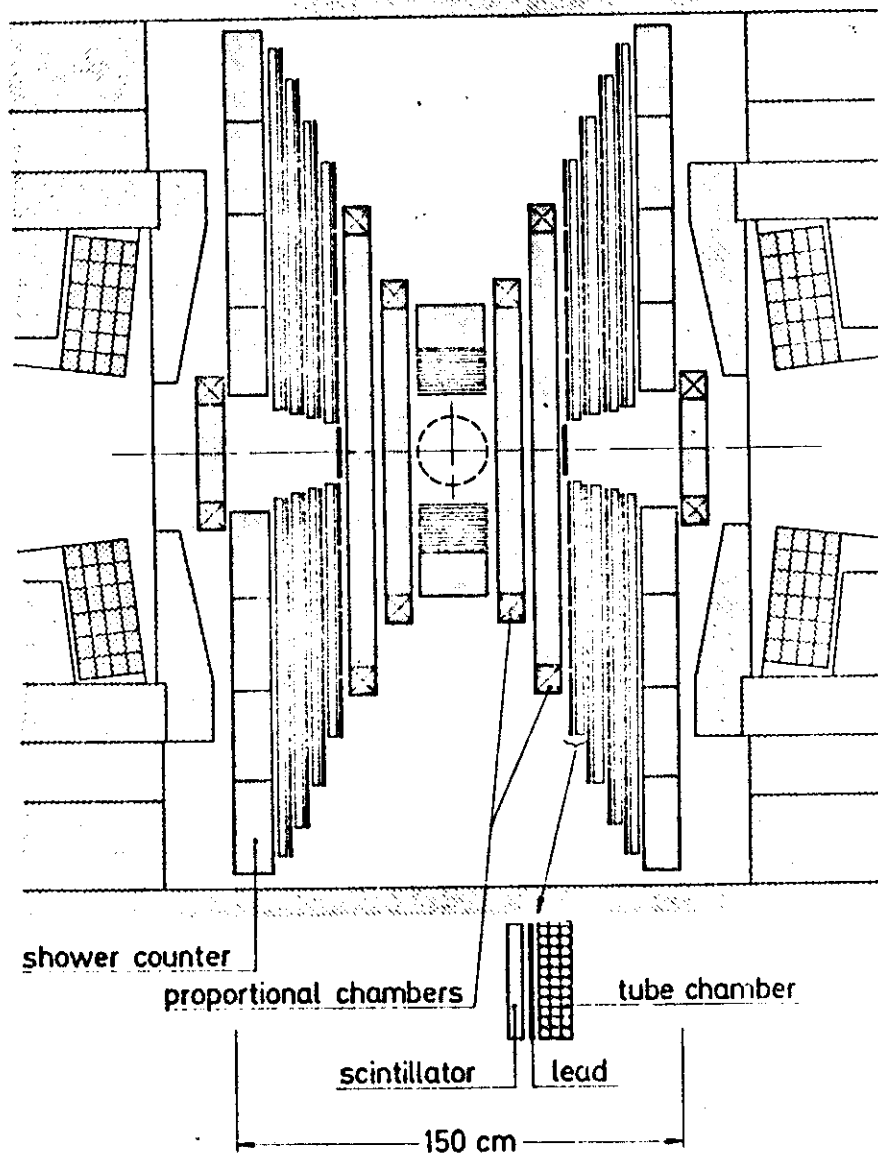
II. Institut für Experimentalphysik der Universität Hamburg

W. de Boer, G. Buschhorn, B. Gunderson, R. Kotthaus, U.E. Kruse⁴, H. Lierl,
H. Oberlack, K. Pretzl, and M. Schliwa,
Max-Planck-Institut für Physik und Astrophysik, München

S. Orito, T. Suda, Y. Totsuka and S. Yamada
University of Tokyo, Tokyo

DASP



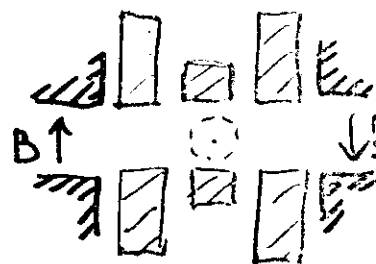


DASP — Inner Detector

fig. 2

Trigger :

6 octants split at $\theta = 90^\circ$
 \Rightarrow 12 segments



Segment trigger

TWO OF THREE — shower counter
 (thresh. = $2 \times$ min. ion. part.) and
 the two preceding scint. — have
 fired

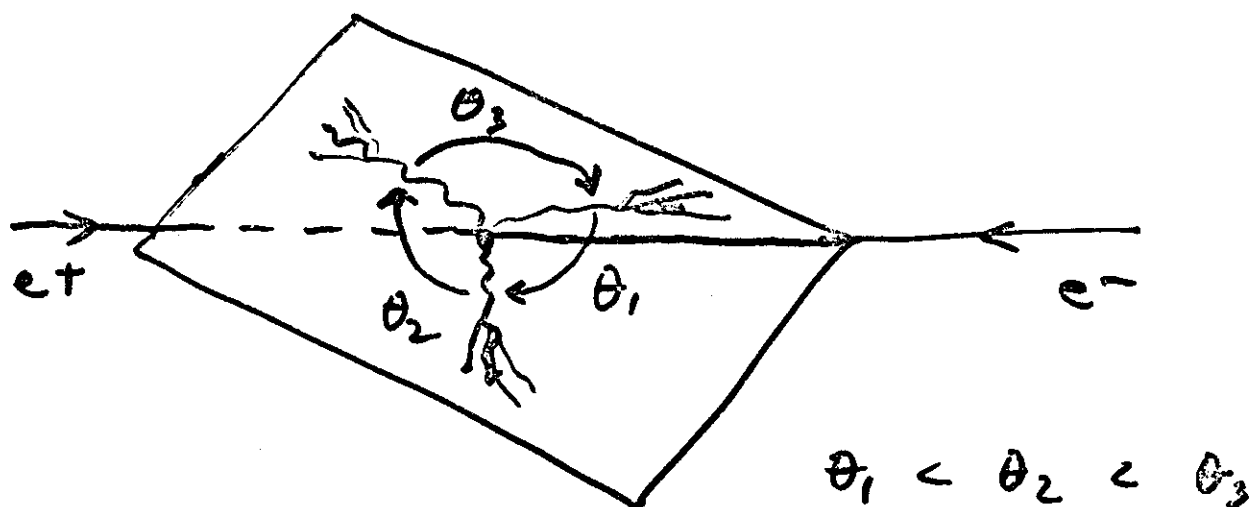
event trigger : OR of

- p.h. $\geq 2 \times$ min. ion. part. in 2 segm.
- p.h. $\geq 1 \times$ min. ion. part. in 3 segm.

Event selection :

- ≤ 1 out of 22 beam pipe counters fire
- $E_{tot} \geq 2 \text{ GeV}$
- $\delta z \leq 24 \text{ cm}$; $\delta t \leq 7 \text{ nsec}$
- 3 and only 3 photon showers
pointing towards int. point (local!)
- $\theta_{\gamma\gamma}^{\text{min}} \geq 30^\circ$ (also excludes $\pi\gamma$)

Kinematical reconstruction



- θ_{γ_i} from conv. pt. and int. pt.
- fit plane to 3 conv. pts. and int. pt. fig. 3
- $\chi^2 < 2.7$: 149 evts. \rightarrow 110 evts.
- calculate E_{γ_i} from θ_{γ_i} and E_{cm}
- calculate $m_{\gamma\gamma}$ from θ_{γ_i} (=meas.) and E_{γ_i} (=calc.)

$$\Delta m_{\gamma\gamma} : \underset{(\gamma)}{24 \text{ MeV}} - \underset{(X)}{40 \text{ MeV}}$$

$$e^+e^- \rightarrow 3\gamma \text{ at } \sqrt{s}=3.1 \text{ GeV}$$

least square fit

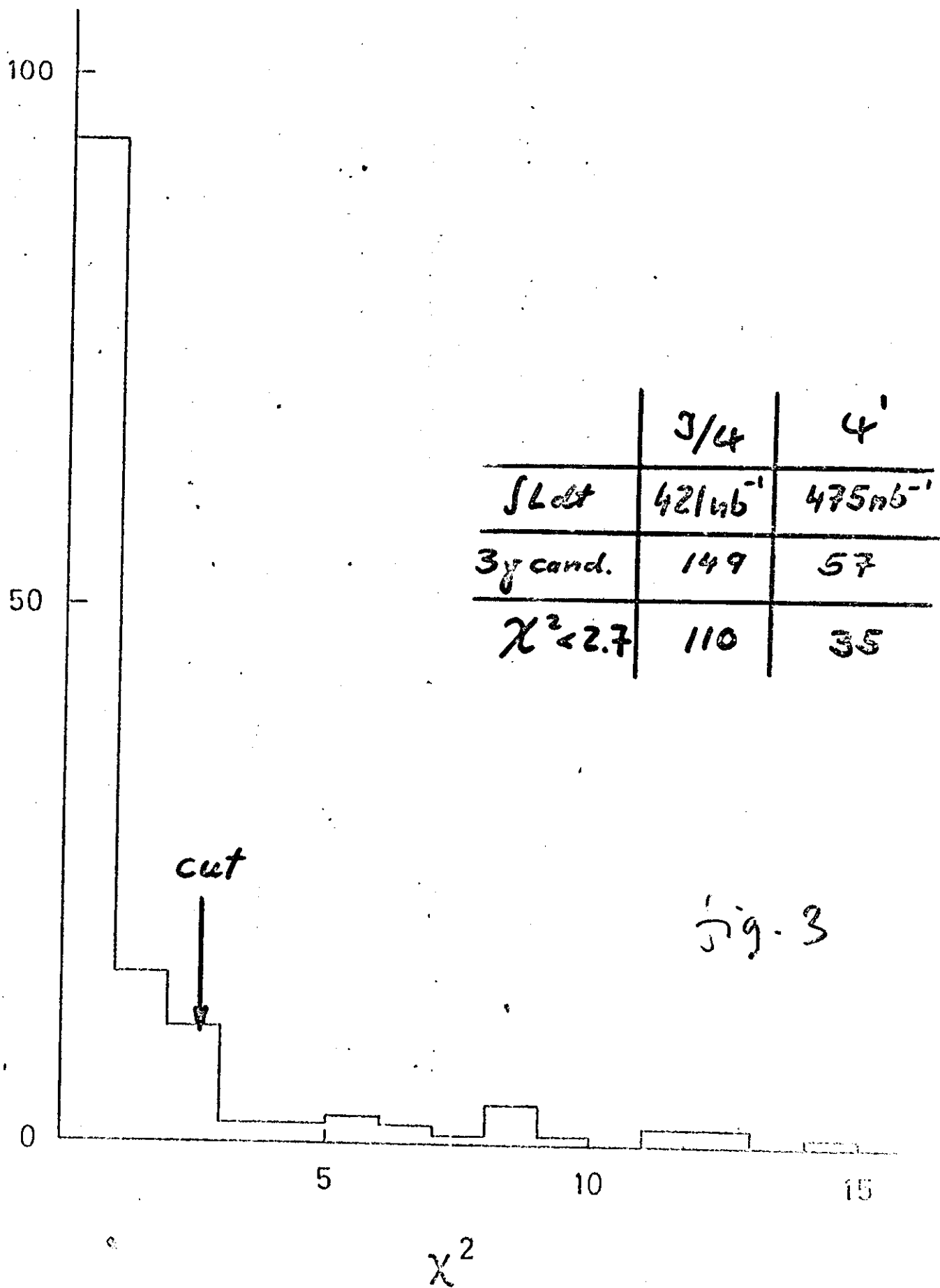


Fig. 3

Background

QED:

- use matrix elements from
Behrend & Gastman to calculate
 $E_{\gamma_i} (\approx \theta_{\gamma_i})$
- MC: shower development
photon acc. and effie.
- analyse MC-events like real
events

ϵ_{12}

by MC from measured yield

Results :

1. 4 σ -effect for $J/\psi \rightarrow \gamma(X \rightarrow 2\gamma)$ fig. 4a,b,c

$$2.8 < m_X < 2.9 \text{ GeV}$$

$$BR(J/\psi \rightarrow \gamma(X \rightarrow 2\gamma)) \approx 1.6 \cdot 10^{-4}$$

$$\Gamma(\quad) \approx 11 \text{ eV}$$

$J_X \neq 1$, $C_X = +1$ a good cand. for " ψ_c "

2. hint for $\psi' \rightarrow \gamma X$ fig. 5a,b
3. Summary fig. 6

Comments :

1. status of DESY-Heidelberg - analysis: not yet fin. (multiplicity?)
2. X not yet seen in any other decay mode !!
e.g. $X \rightarrow p\bar{p}$

$$BR(J/\psi \rightarrow \gamma(X \rightarrow p\bar{p})) \begin{cases} < 2 \cdot 10^{-4} & \text{DRSP} \\ < 5 \cdot 10^{-5} & \text{SLAC/UC} \end{cases}$$

M_{\min}^2 vs. M_{\max}^2 for $e^+e^- \rightarrow \gamma\gamma\gamma$ at 3.1 GeV

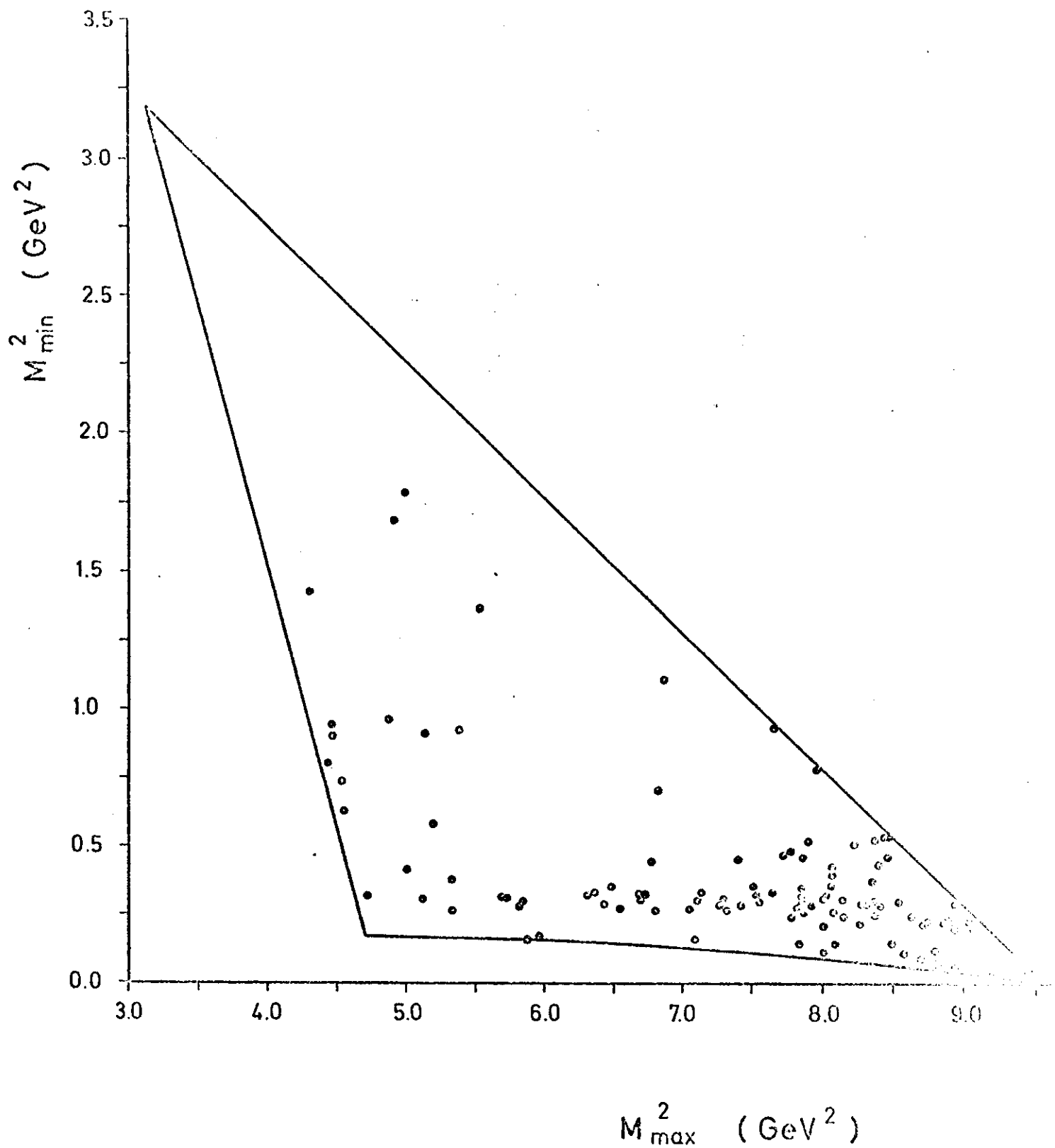


Fig. 4a

$e^+e^- \rightarrow \gamma\gamma\gamma$ at $\sqrt{s}=3.1$ GeV

Low mass solution

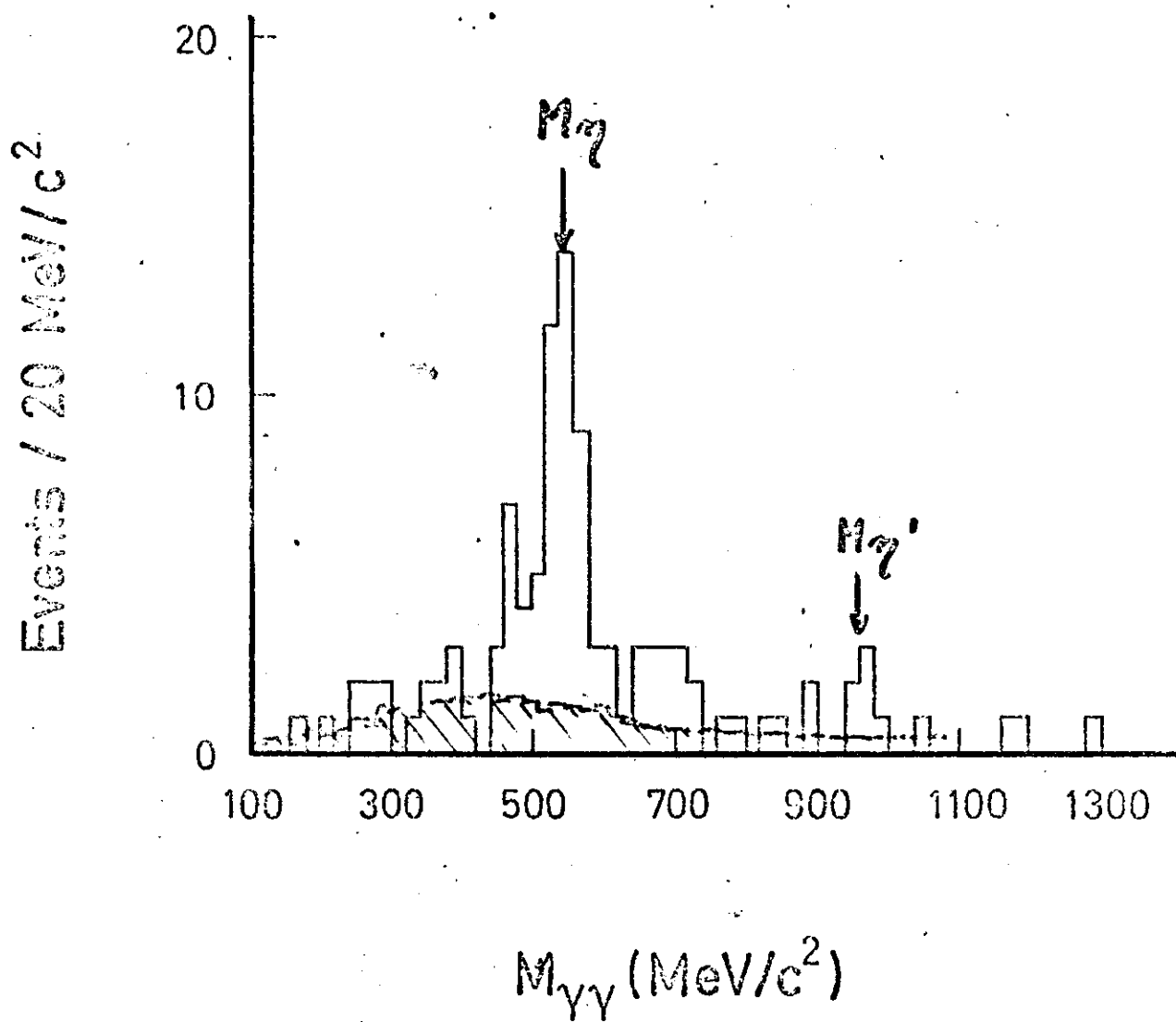


Fig. 4b

$e^+e^- \rightarrow \gamma\gamma\gamma$ at $\sqrt{s}=3.1$ GeV

High mass solution

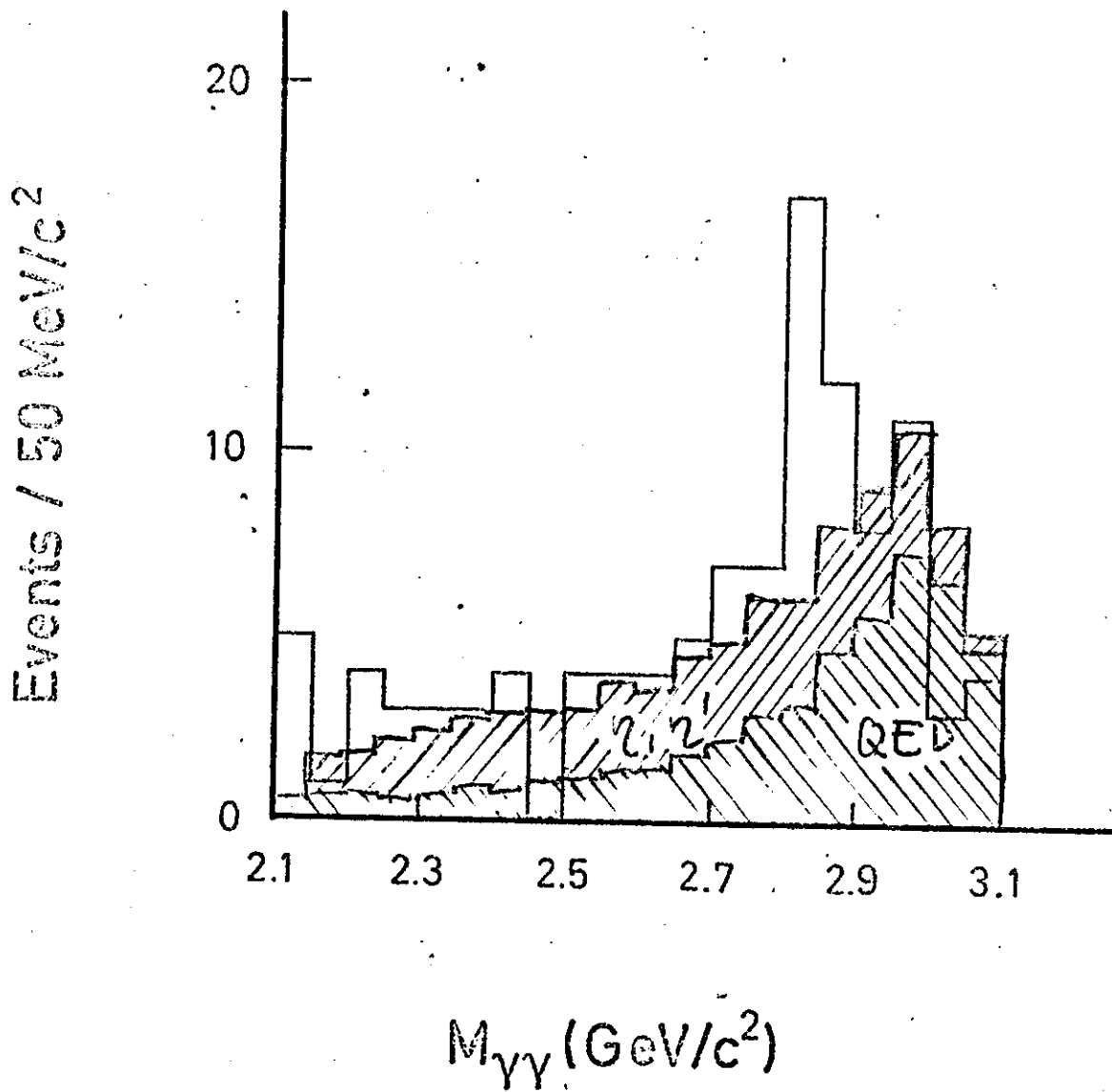


fig. 4c

M_{\min}^2 vs. M_{\max}^2 for $e^+e^- \rightarrow \gamma\gamma\gamma$ at 3.7 GeV

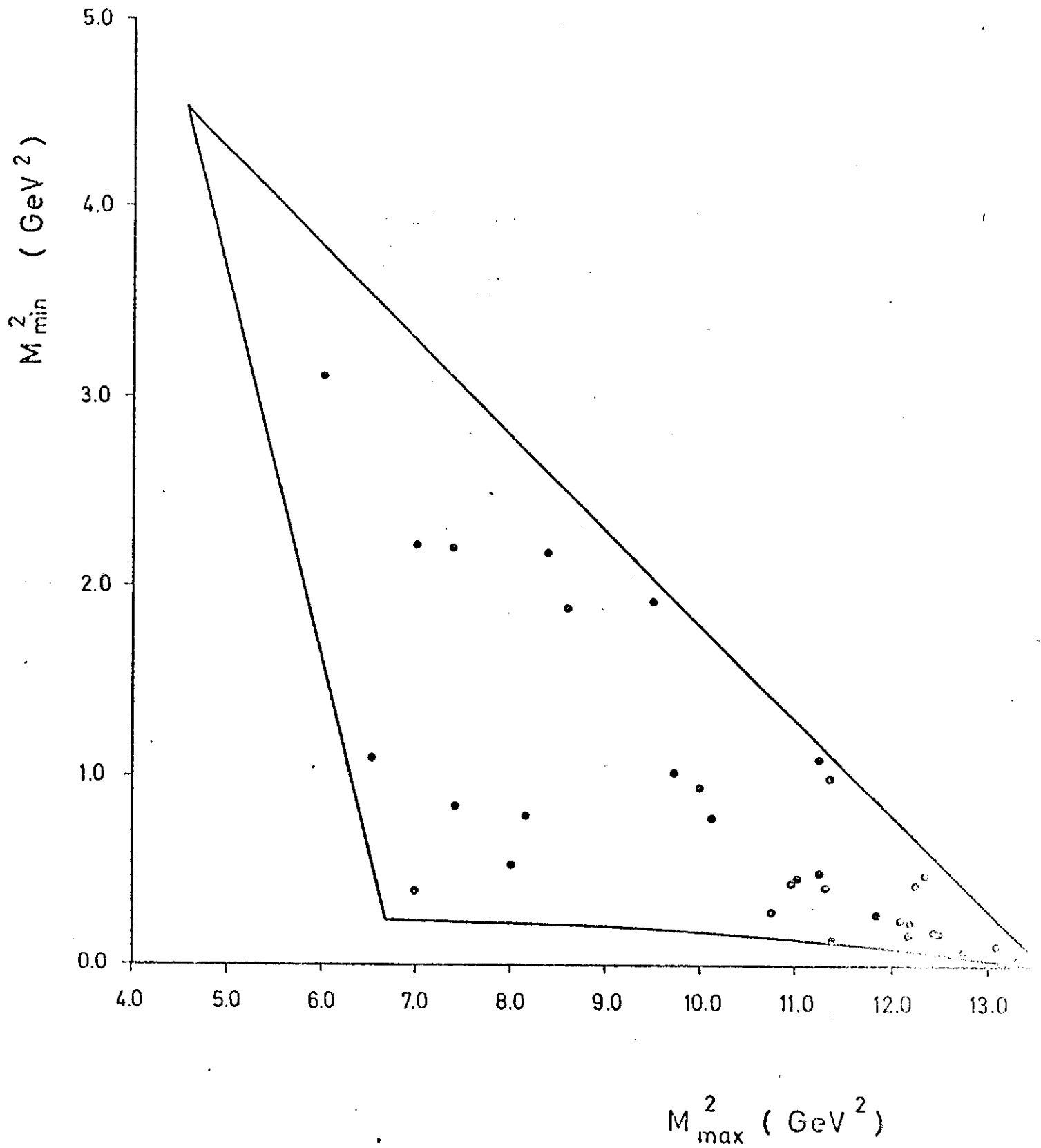


Fig. 5a

$e^+ e^- \rightarrow \gamma\gamma\gamma$ at $\sqrt{s} = 3,7$ GeV

High mass solution

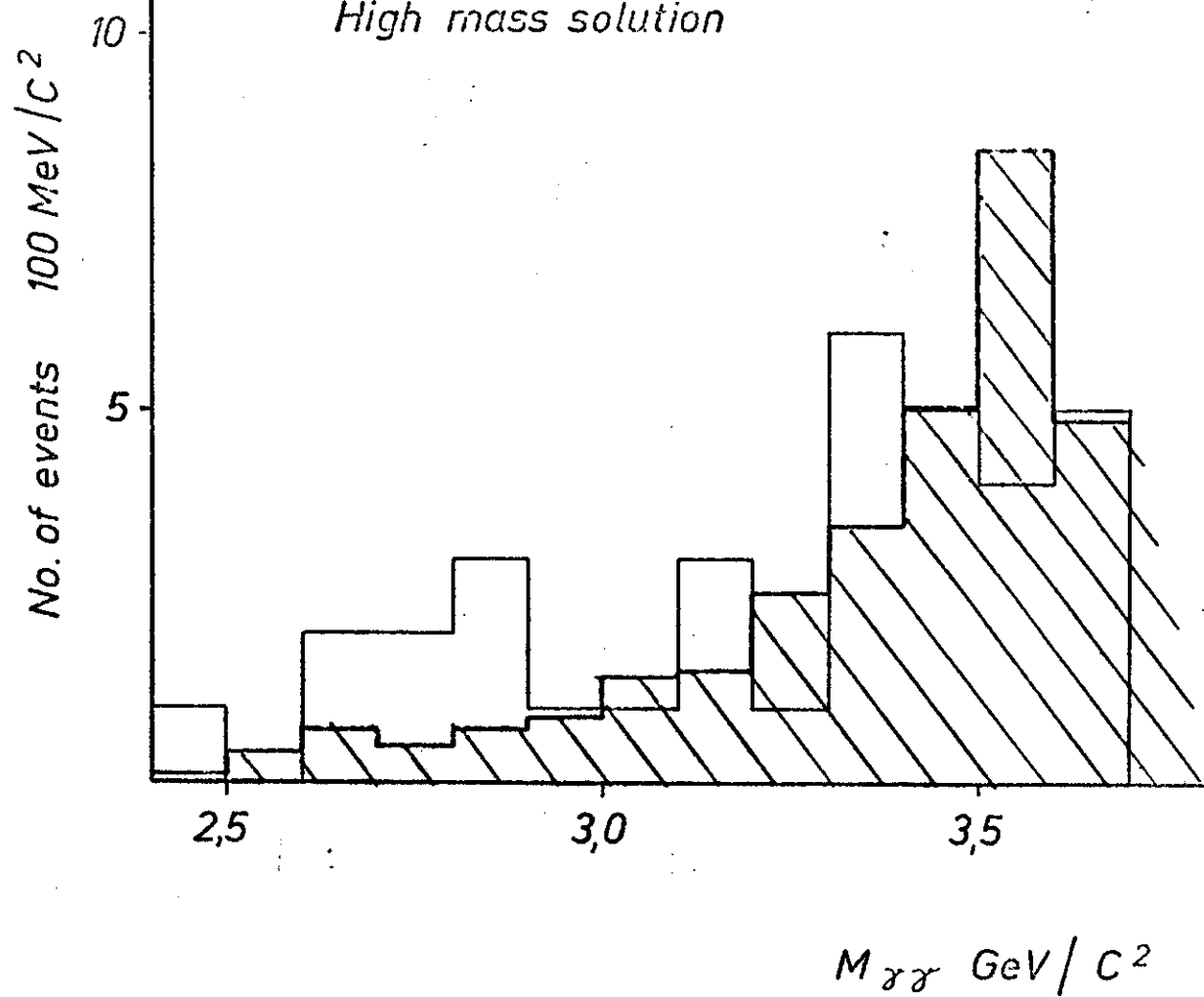


Fig. 56

Summary of $J/\psi, \psi' \rightarrow 3\gamma$ (DASP)

		J/ψ	ψ'
$\eta\gamma$	Γ	$69 \pm 14 \text{ eV}$	$< 300 \text{ eV}$
	BR	$(1.0 \pm 0.2) \cdot 10^{-3}$	$< 1.3 \cdot 10^{-3}$
$\eta'\gamma$	Γ	$< 300 \text{ eV}$	$< 3.15 \text{ keV}$
	BR	$< 4.4 \cdot 10^{-3}$	$< 1.4 \cdot 10^{-2}$
$\gamma(K \rightarrow 2\gamma)$	Γ	$\sim 11 \text{ eV}$	$< 83 \text{ eV}$
	BR	$\sim 1.6 \cdot 10^{-4}$	$< 3.7 \cdot 10^{-4}$
$\gamma(\rho_c \rightarrow 2\gamma)$	Γ		$< 302 \text{ V}$
	BR		$< 1.3 \cdot 10^{-4}$

fig. 6

P_c / X

1. DASP

$$\psi' \rightarrow \gamma P_c$$

$$\hookrightarrow \gamma + (J/\psi \rightarrow \mu\mu)$$

fig. 7 : $E_{\gamma_1} - E_{\gamma_2}$

fig. 8 : Compar. DASP-SLAC/CLE

2. DESY-Heidelberg

$$\psi' \rightarrow \gamma P_c$$

$$\hookrightarrow \gamma + (J/\psi \rightarrow \mu\mu_{ee})$$

Detector : NaJ - Pb glass det.

fig 9, 10, 11 with drift-ch. core-detector
and μ -detection

E_γ - distr. (av. over P_c) fig. 12

θ_γ - distr. (") fig. 11

$$\gamma_1 : W(\theta) \sim 1 - (1.1 \pm 0.3) \cos^2 \theta$$

γ_2 : isotropic

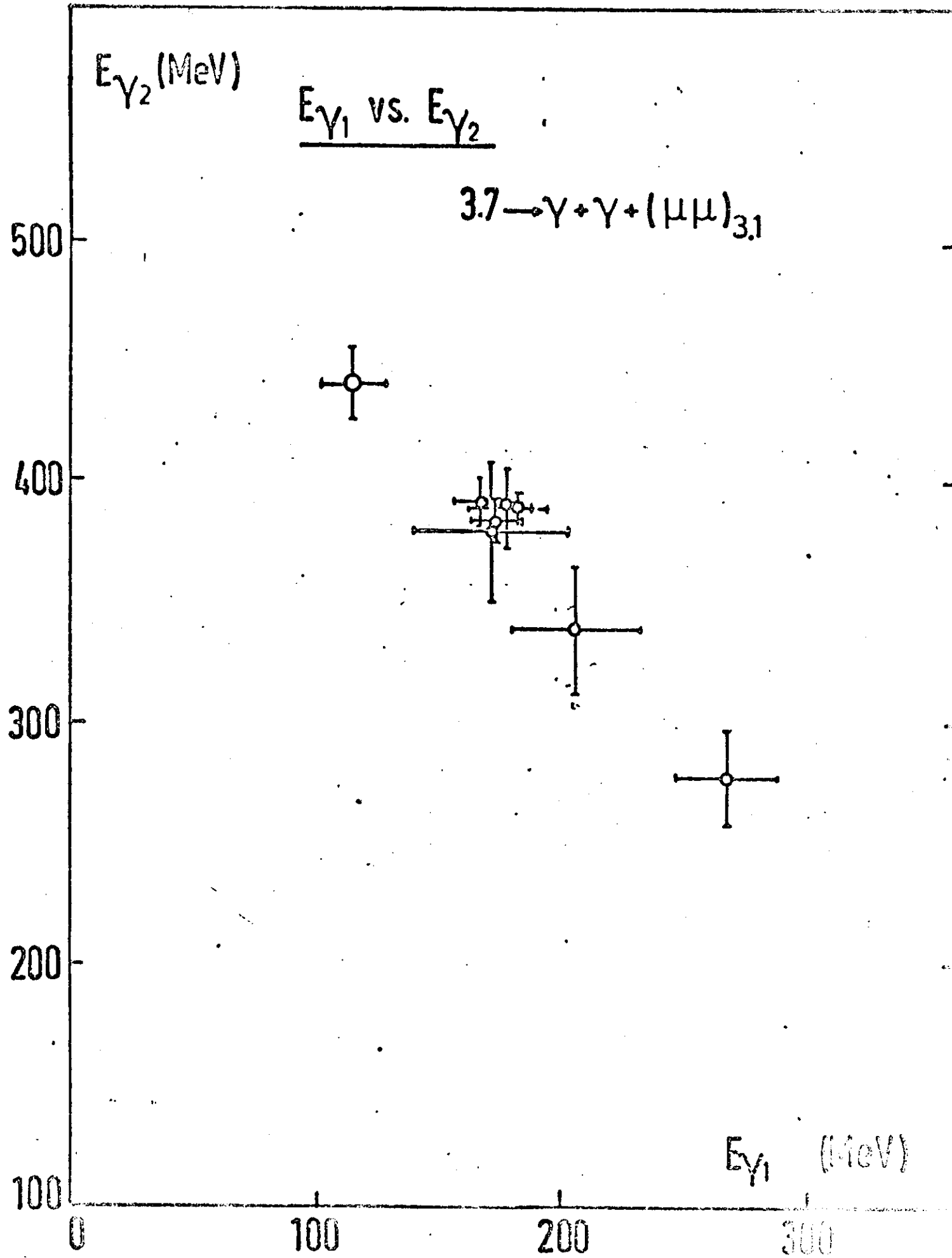


fig. 7

P_c / χ

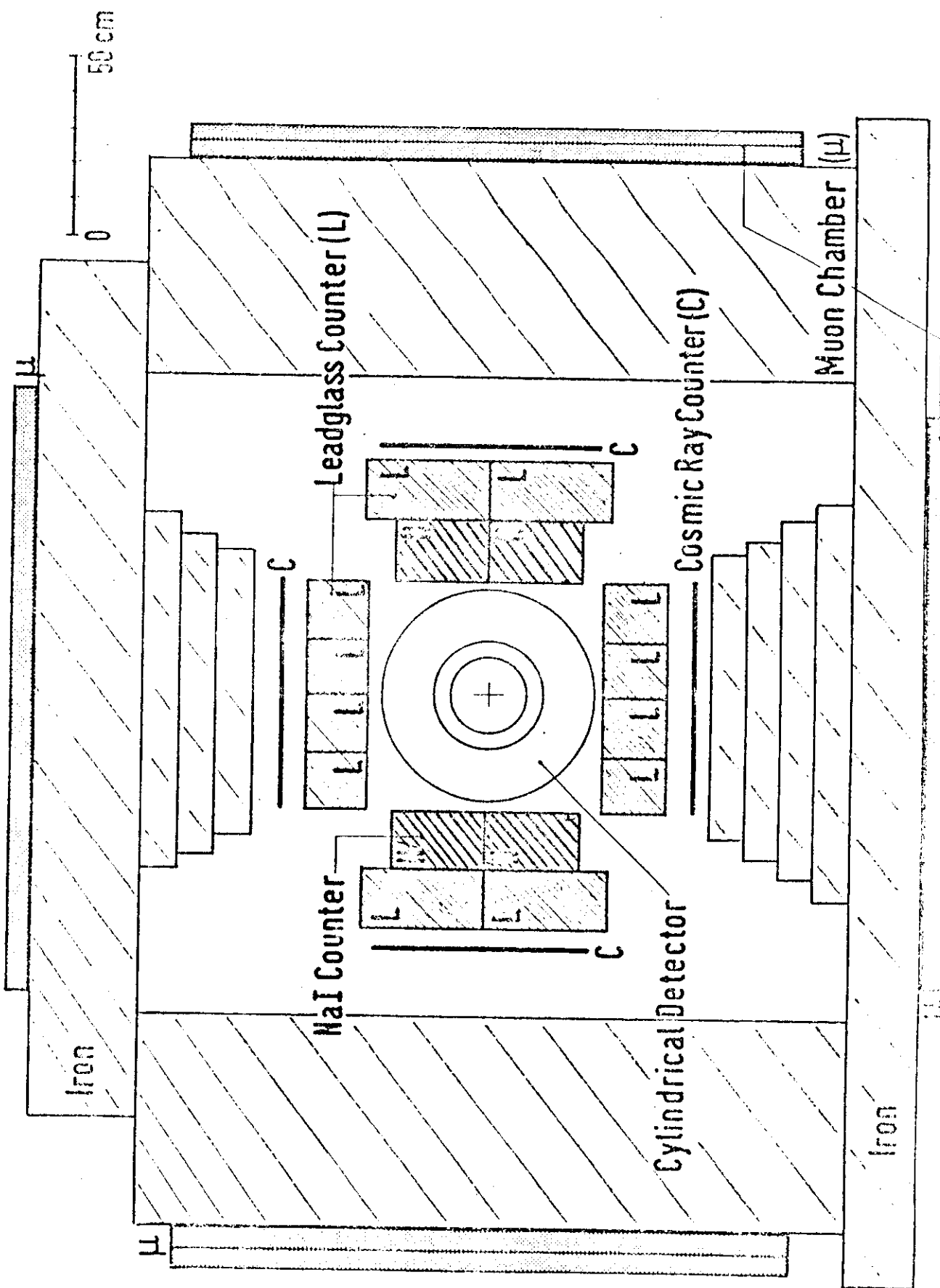
	$m_{P_c} \text{ (GeV)}$	# evts	$BR(\psi' \rightarrow \gamma P_c)(P_c \rightarrow \gamma J/\psi)$
D	3.55	1	.01
S	3.55	4	$.01 \pm .005$
D	3.50	5	$\sim .04 \pm .02$
S	3.50	12	$.03 \pm .01$
D	3.46	1	$\sim .01$
S	3.45	4	$.01 \pm .005$
D	3.40	1	$\sim .01$
S	3.41	1	$< .008$

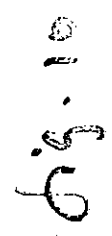
D = DORIS (DASP)

S = SPEAR (SLAC/LBL)

fig. 8

Fig. 9





DESY - Heidelberg

W. Bartel

P. Duinker

J. Heintze

G. Heinzelmann

R.D. Heuer

R. Mundhenke

D. Pandoulas

H. Rieseberg

B. Schünleier *)

P. Steffen

J.E. Olsson

A. Wagner

A.H. Walenta

*) now IDAS

fig. 11

$$\psi'(3.7) \rightarrow \gamma \gamma \quad J/\psi(3.1)$$

$$\rightarrow \begin{pmatrix} e^+ e^- \\ \mu^+ \mu^- \end{pmatrix} \quad \begin{matrix} \textcircled{1} \\ \textcircled{2} \end{matrix}$$

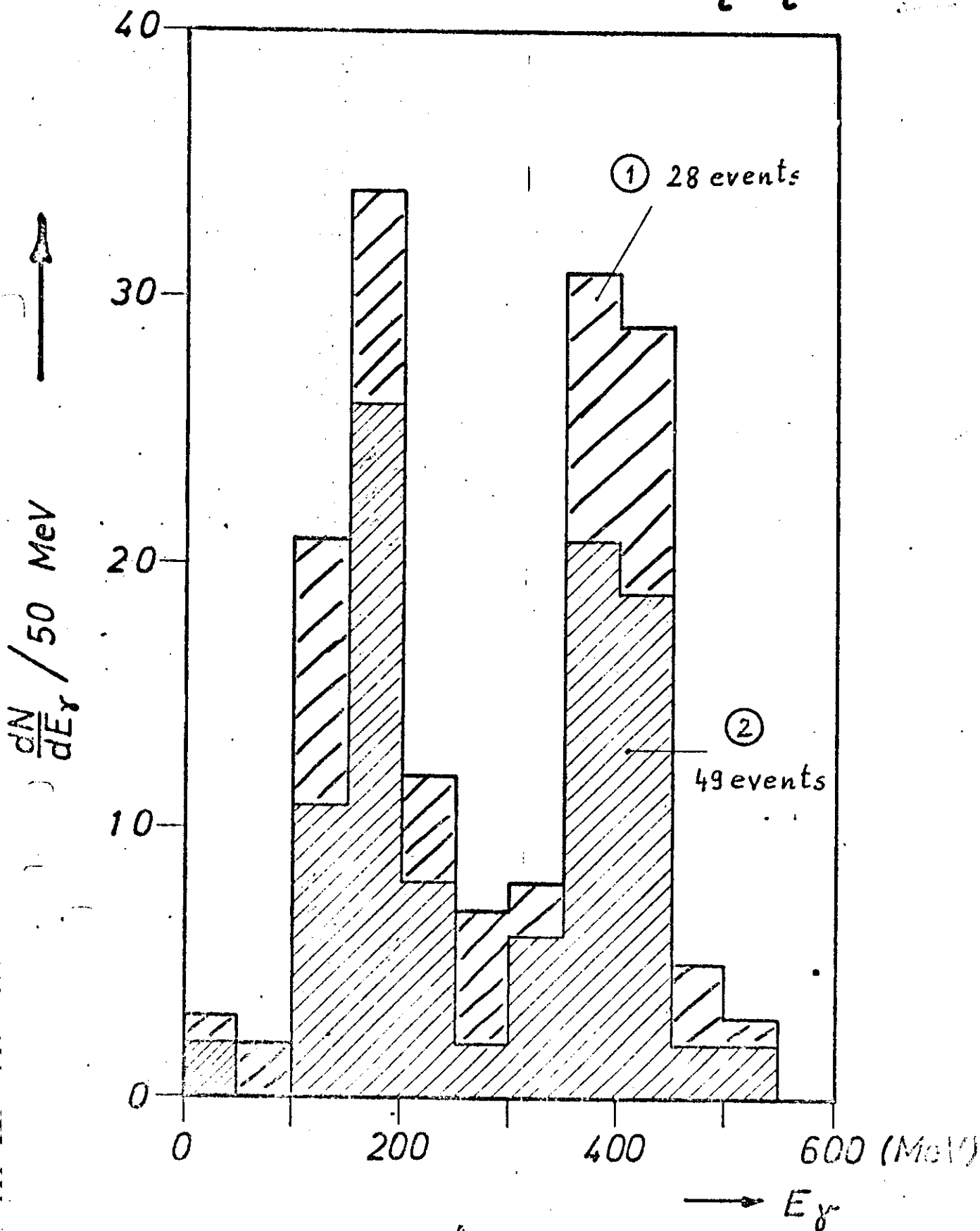


Fig. 12

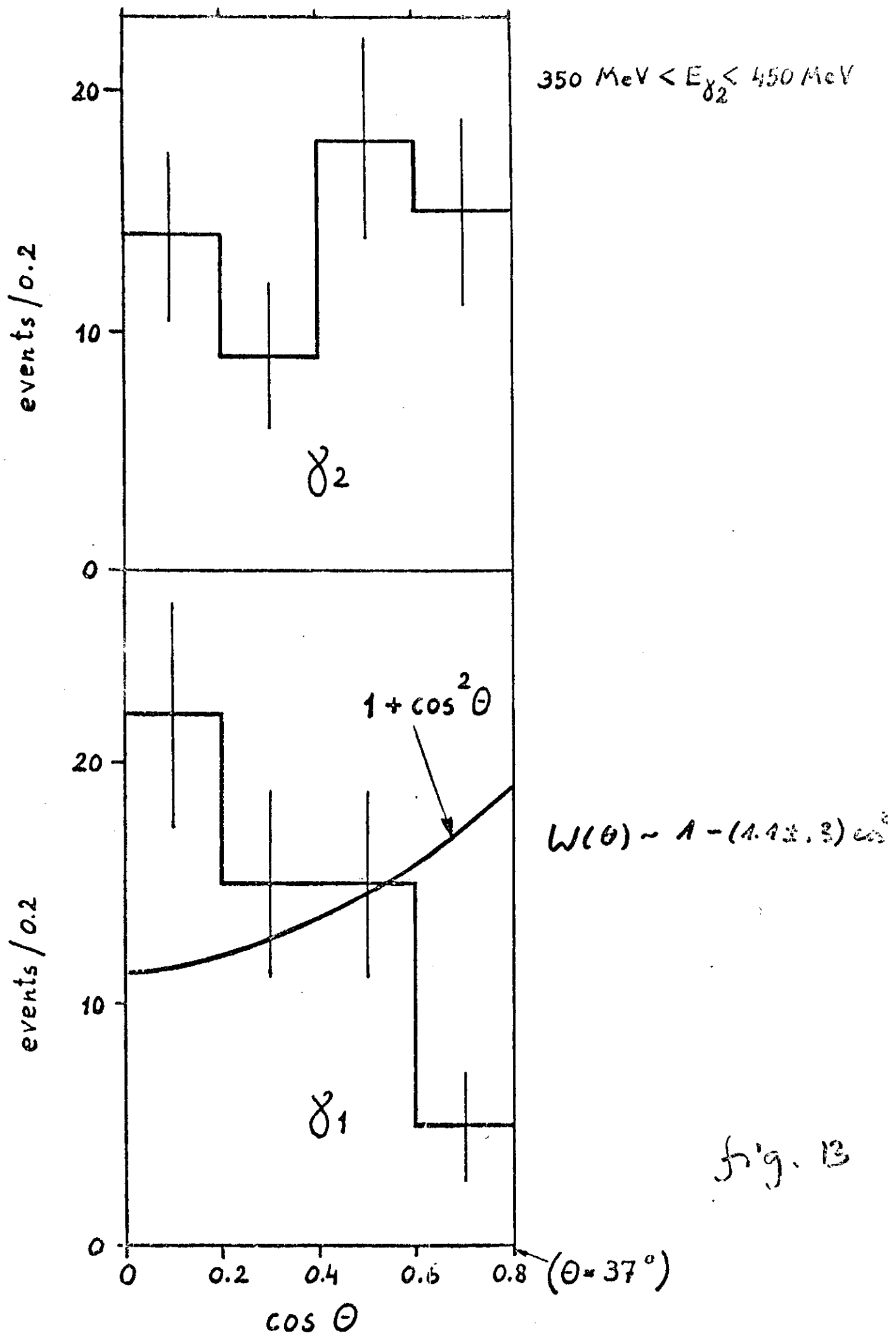


fig. 13

I.3 J/ψ - decay modes

1. DESY - Heidelberg - Coll.

$$J/\psi \rightarrow \pi^+ \pi^- \gamma \gamma \quad (\sim 1100 \text{ evts.})$$

a) $J/\psi \rightarrow \pi^0 \rho^0$
 $\pi^\pm \rho^\mp$ fig. 14 a, b, c

$$BR(J/\psi \rightarrow \pi \rho) = (1.1 \pm 0.2) \cdot 10^{-2} \quad \text{D-Hd}$$

$$\left[\begin{array}{ll} (1.3 \pm 0.3) \cdot 10^{-2} & \text{SLAC/CLEO} \\ (1.2 \pm 0.3) \cdot 10^{-2} & \text{DASP} \end{array} \right]$$

$$\frac{\Gamma(J/\psi \rightarrow \pi^0 \rho^0)}{\Gamma(J/\psi \rightarrow \pi^\pm \rho^\mp)} = 0.6 \pm 0.2 \quad \sim \frac{\Gamma_{\pi^0 \rho^0}}{\Gamma_{J/\psi}} = 0$$

b) $J/\psi \rightarrow \gamma(\eta' \rightarrow \rho \gamma)$ fig. 14 d

$$BR(J/\psi \rightarrow \gamma \eta') = (3.3 \pm 1.0) \cdot 10^{-3} \quad \text{D-Hd}$$

$$\left[\begin{array}{ll} < 4.4 \cdot 10^{-3} & \text{DASP(2)} \\ (0.5 - 3.0) \cdot 10^{-3} & \text{DASP(1)} \end{array} \right]$$

$$\left[BR(J/\psi \rightarrow \gamma \eta) = (1.0 \pm 0.2) \cdot 10^{-3} \quad \text{DASP} \right]$$

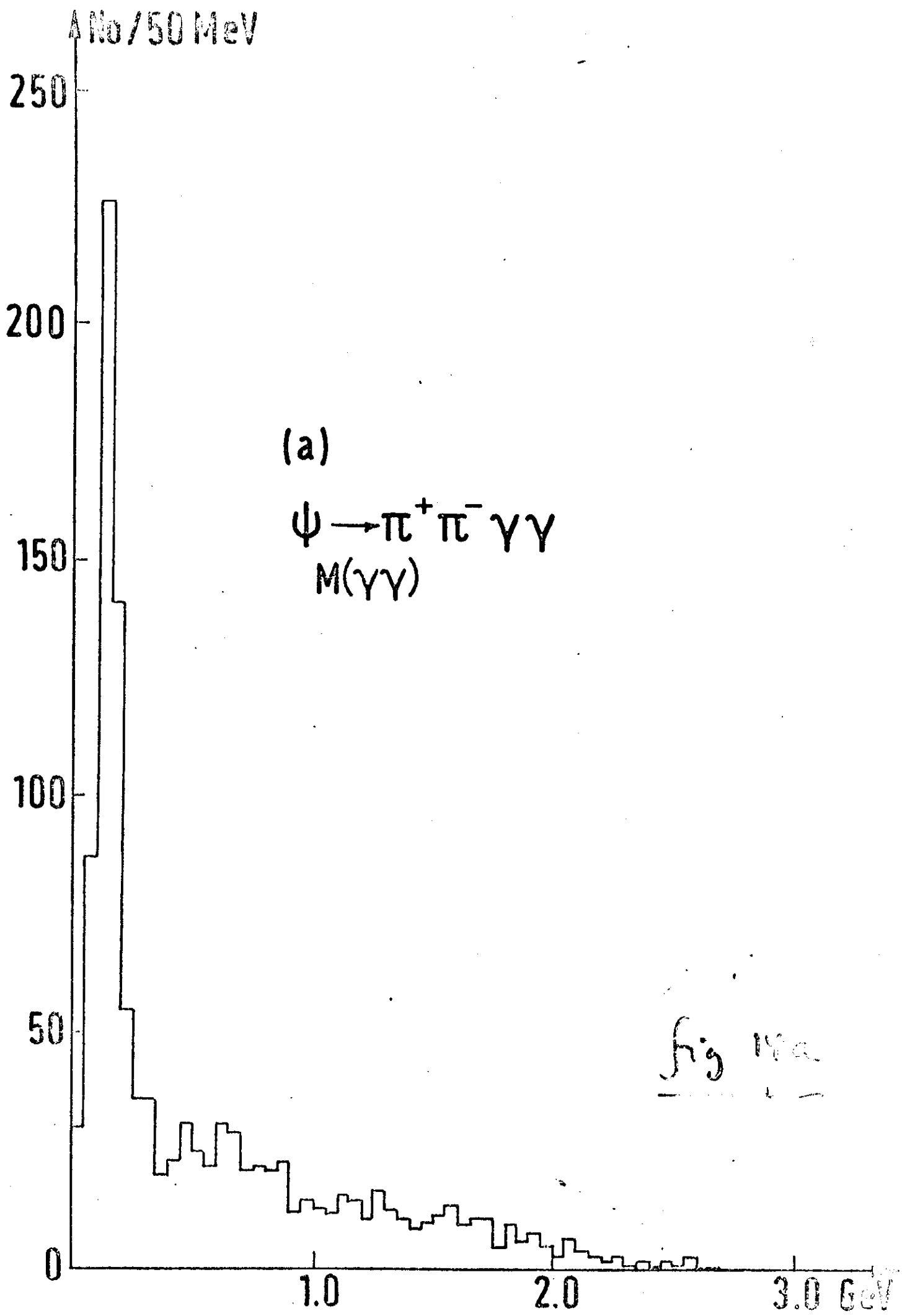
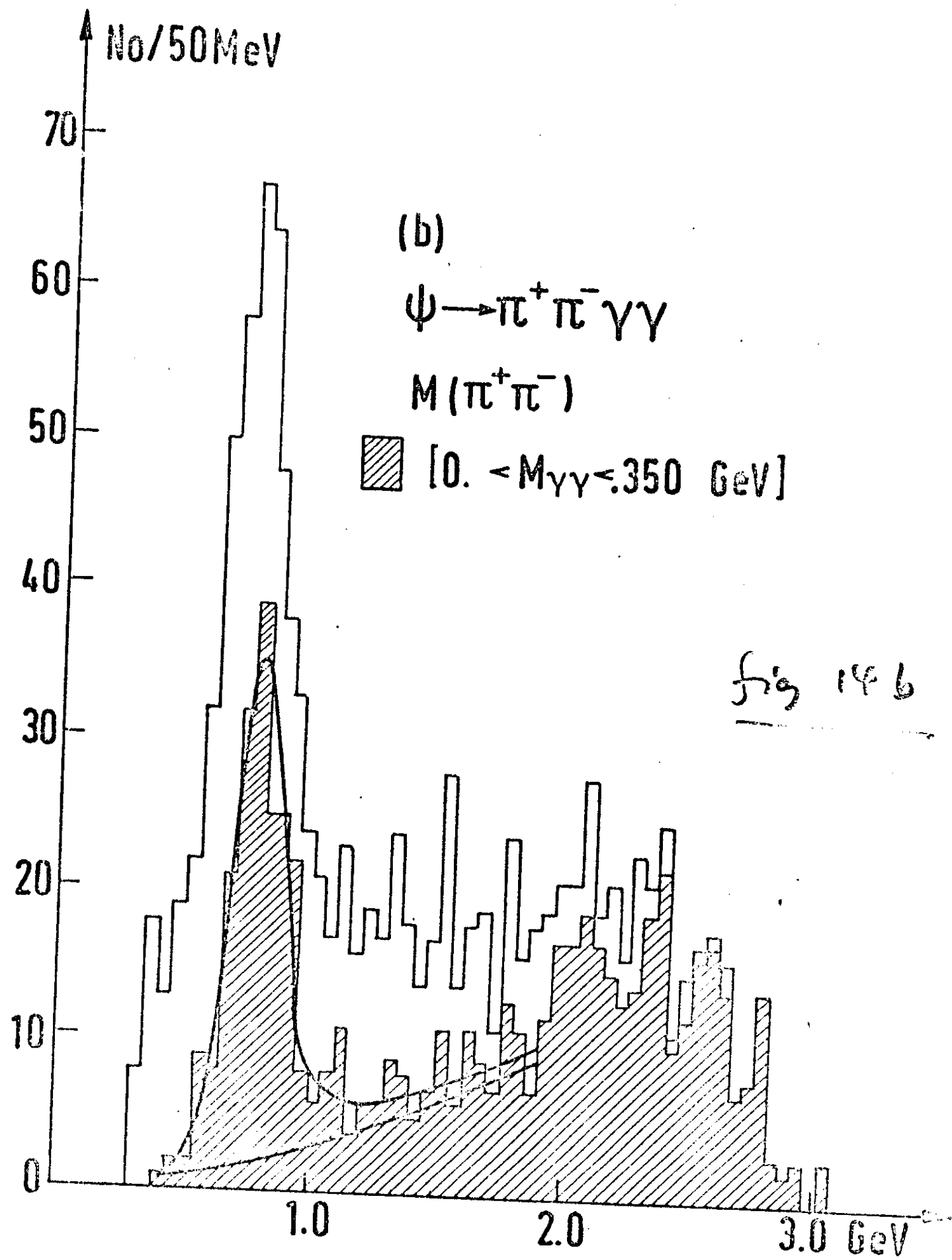


fig 14a



No/50 MeV

90

(c)

$\psi \rightarrow \pi^+ \pi^- \gamma \gamma$

80

$M(\pi^\pm \gamma \gamma)$ 2 entries/event

70

$[0. \leq M_{\gamma\gamma} \leq 0.350 \text{ GeV}]$

60

50

40

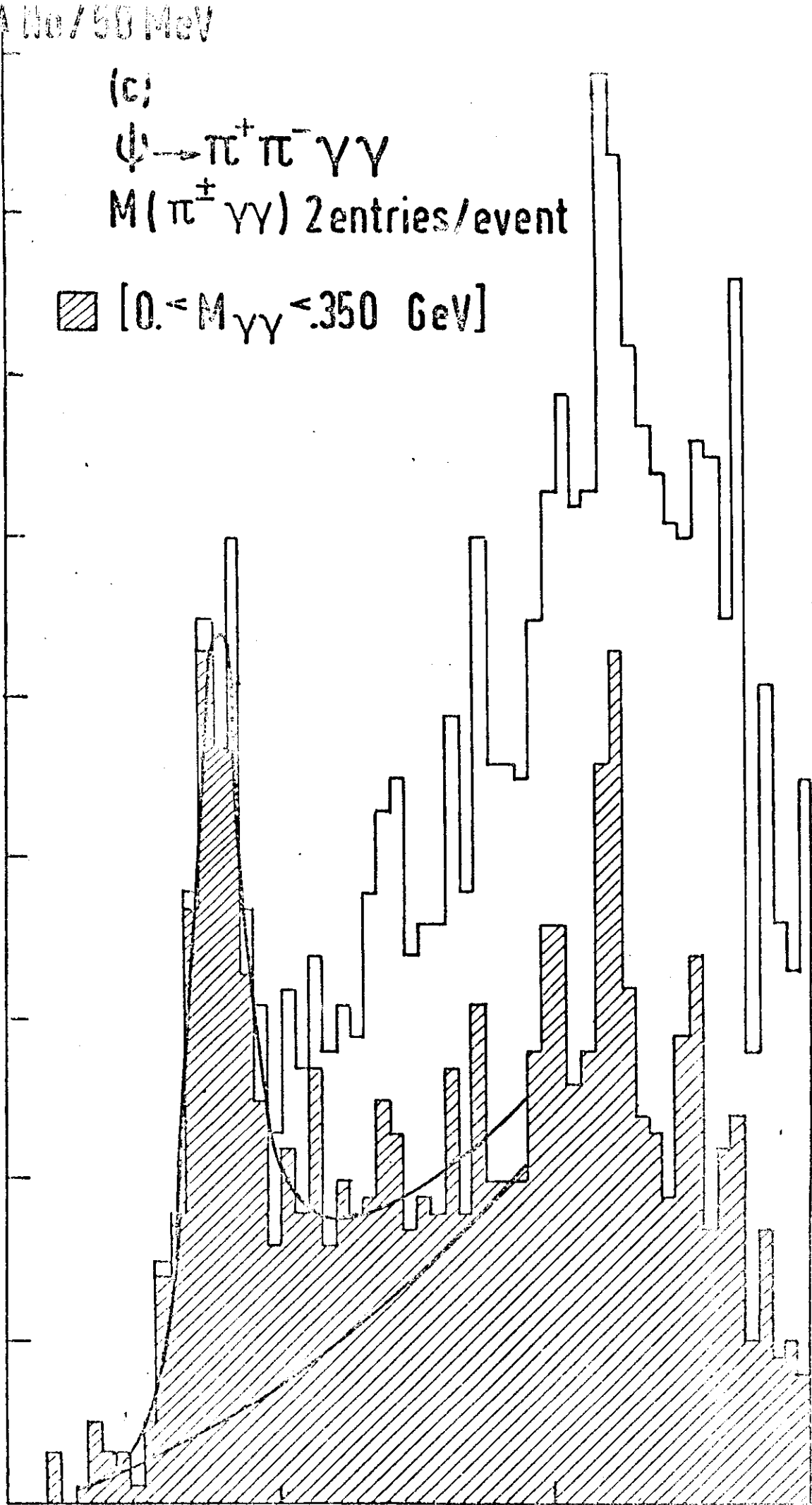
30

20

10

0

Fig. 10

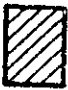


100 — No/50 MeV

(d)

$$\psi \rightarrow \pi^+ \pi^- \gamma \gamma$$

80 — $M(\pi^+ \pi^- \gamma)$ 2 entries/event

 $[.55 < M_{\pi^+ \pi^-} < 1.00 \text{ GeV}]$
 $[M_{\gamma\gamma} < .35 \text{ GeV}]$

60 —

40 —

20 —

0 —

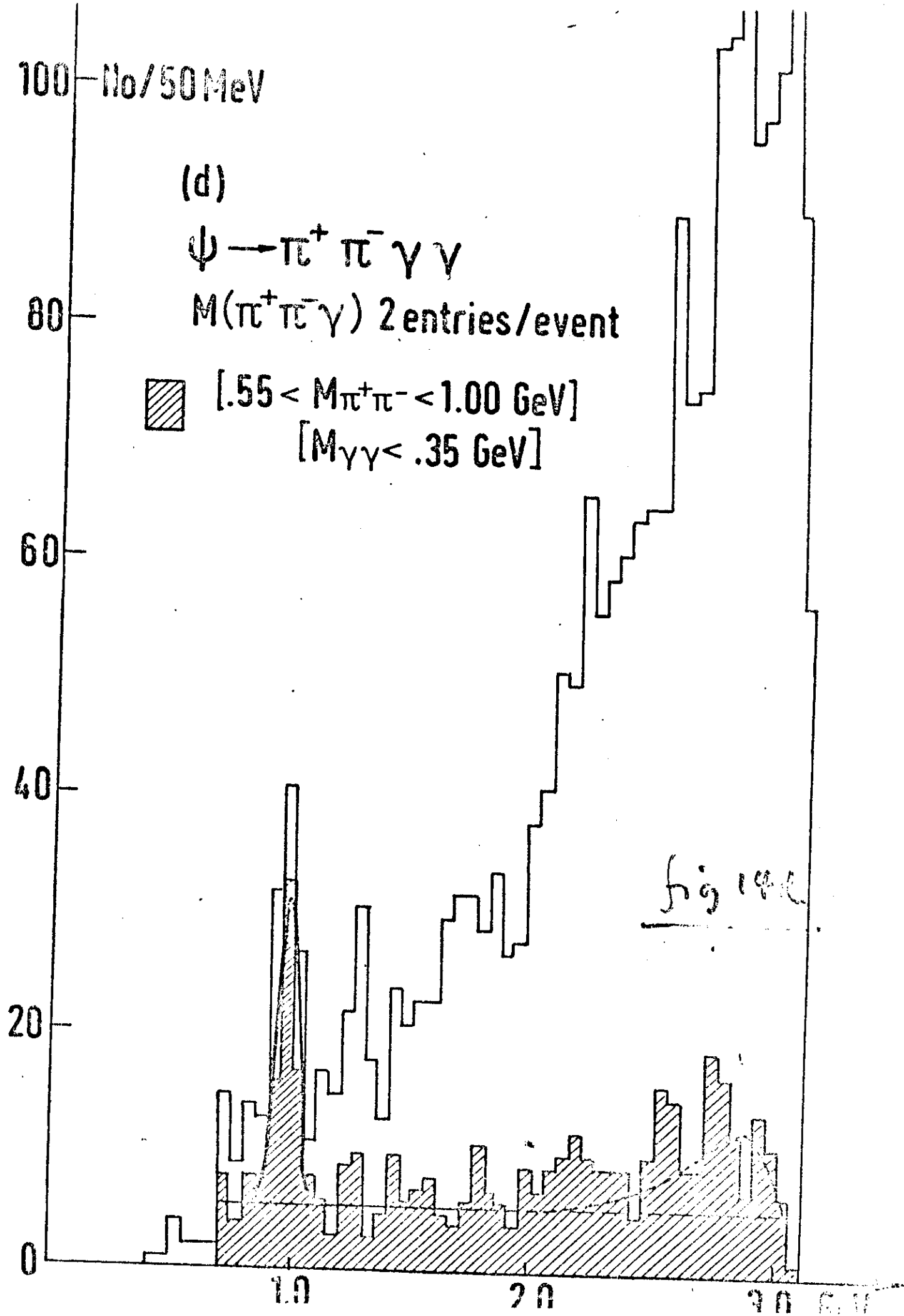
1.0

2.0

3.0

GeV

Fig 14c



2. PLUTO - Coll.

$$J/\psi \rightarrow \pi^+ \pi^- \pi^+ \pi^- X$$

fig 15a, b

$$m_X^2 \approx 0 \Rightarrow X = \pi^0 \text{ or } \gamma$$

$$- BR(J/\psi \rightarrow \pi^+ \pi^- \pi^+ \pi^- \pi^0) = 5.2 \pm 0.2 \%$$

$$[SLAC/LBL : 4.0 \pm 1.0 \%]$$

$$- \omega : M_\omega = 784 \pm 4 \text{ MeV} \quad \text{fig 15c}$$

$$\sigma_{M_\omega} = 36 \pm 5 \text{ MeV}$$

$$\frac{\omega \pi^+ \pi^-}{\pi^+ \pi^- \pi^+ \pi^- \pi^0} = 11 \%$$

$$[SLAC/LBL : 20 \%]$$

- excess of π^0 -momentum at small p_{π^0} fig 15d

$$\frac{\pi^+ \pi^- \pi^+ \pi^-}{\pi^+ \pi^- \pi^+ \pi^- \pi^0} \approx \frac{1}{7}$$

$$[SLAC/LBL \quad \frac{4\pi + 2\pi^0}{\pi^+ \pi^- \pi^+ \pi^- \pi^0} \sim \frac{1}{5}]$$

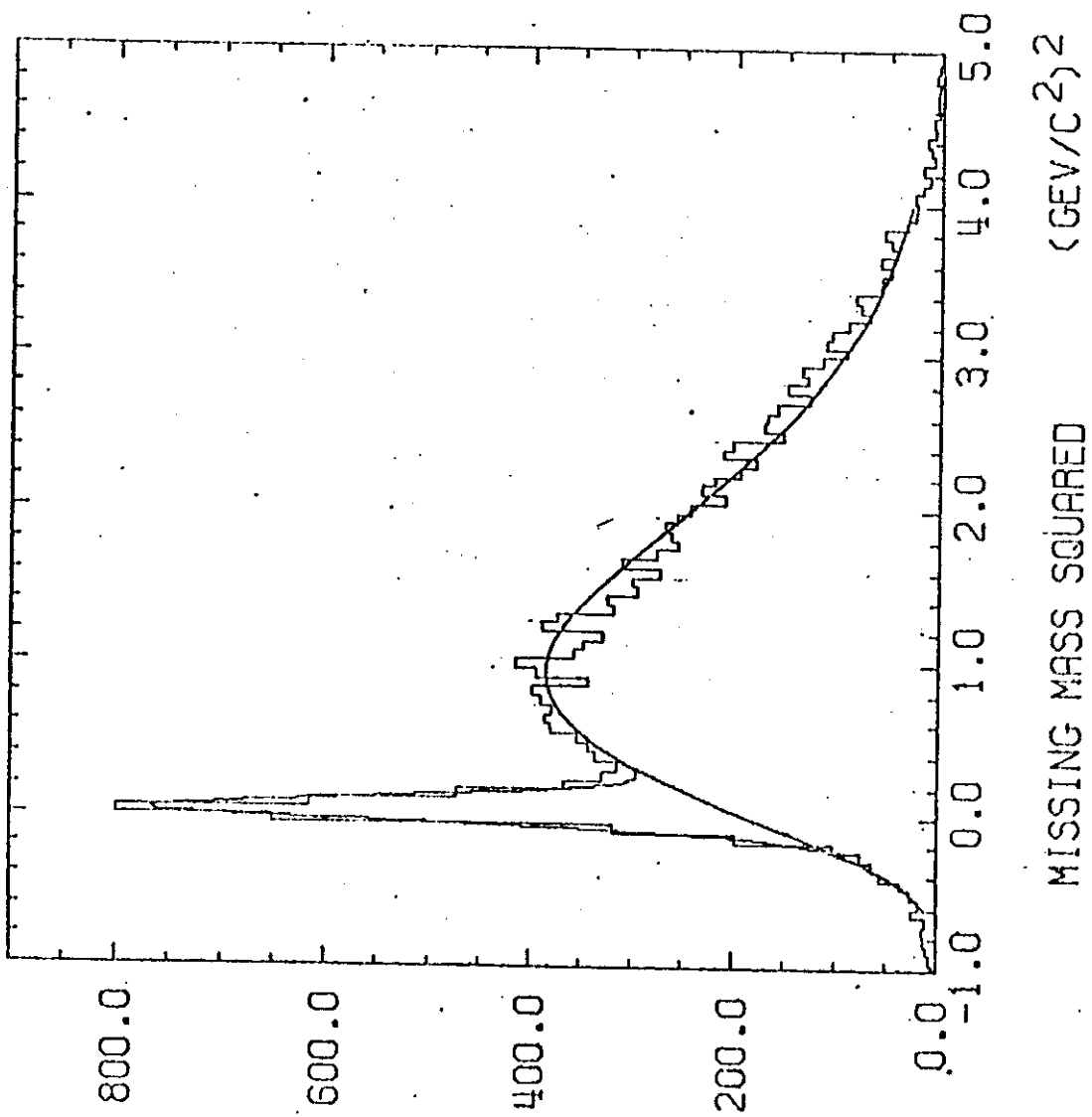
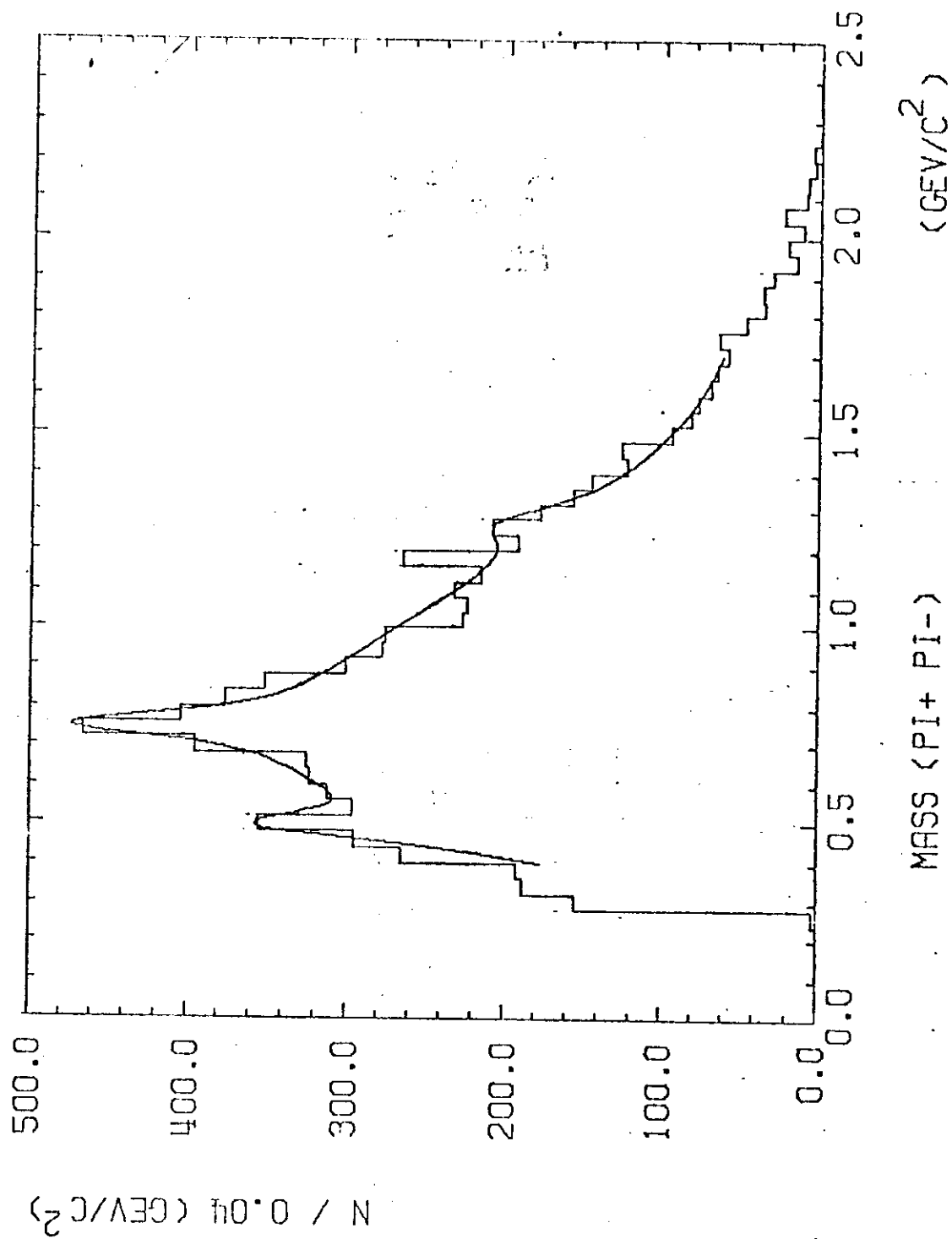
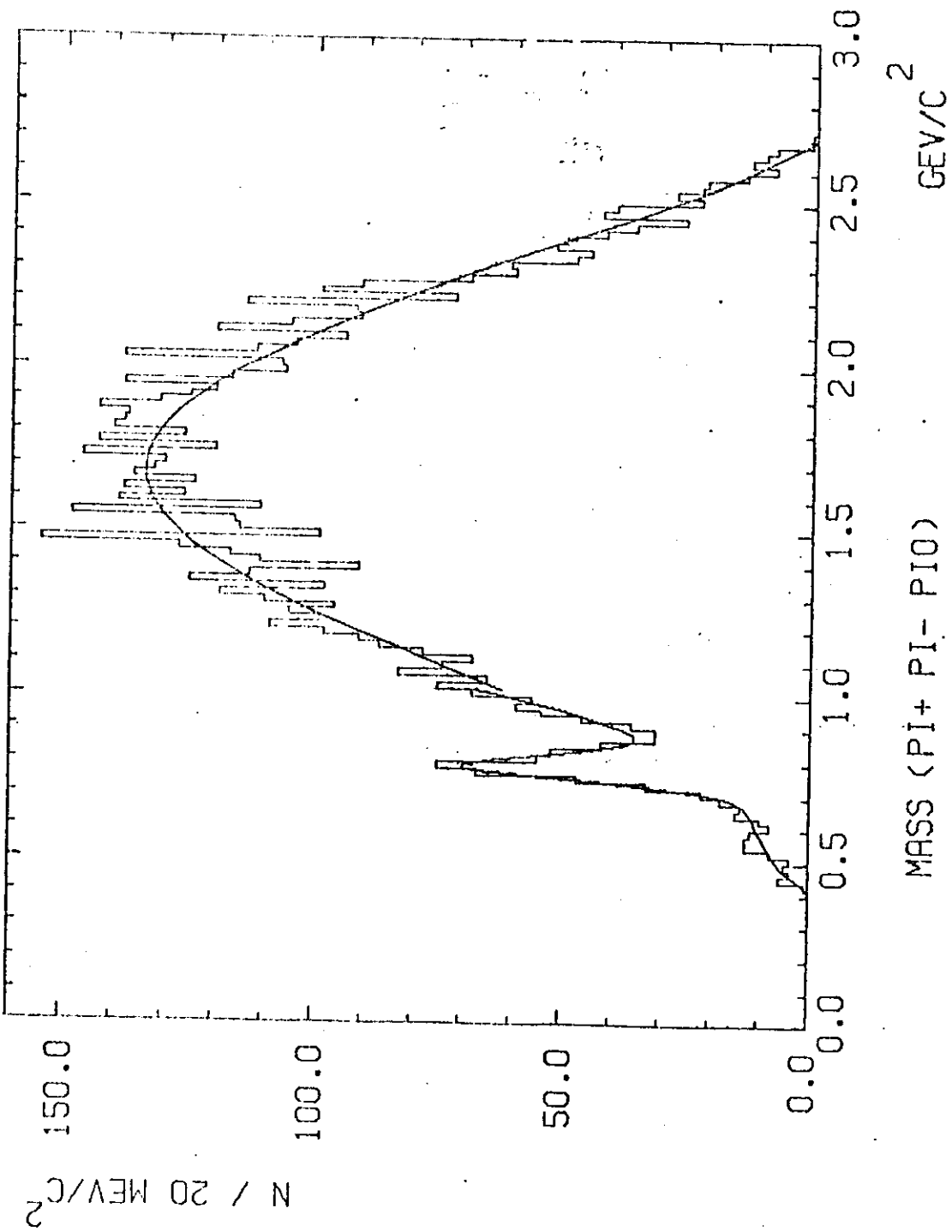


Fig 15a





-991-

fig 15c

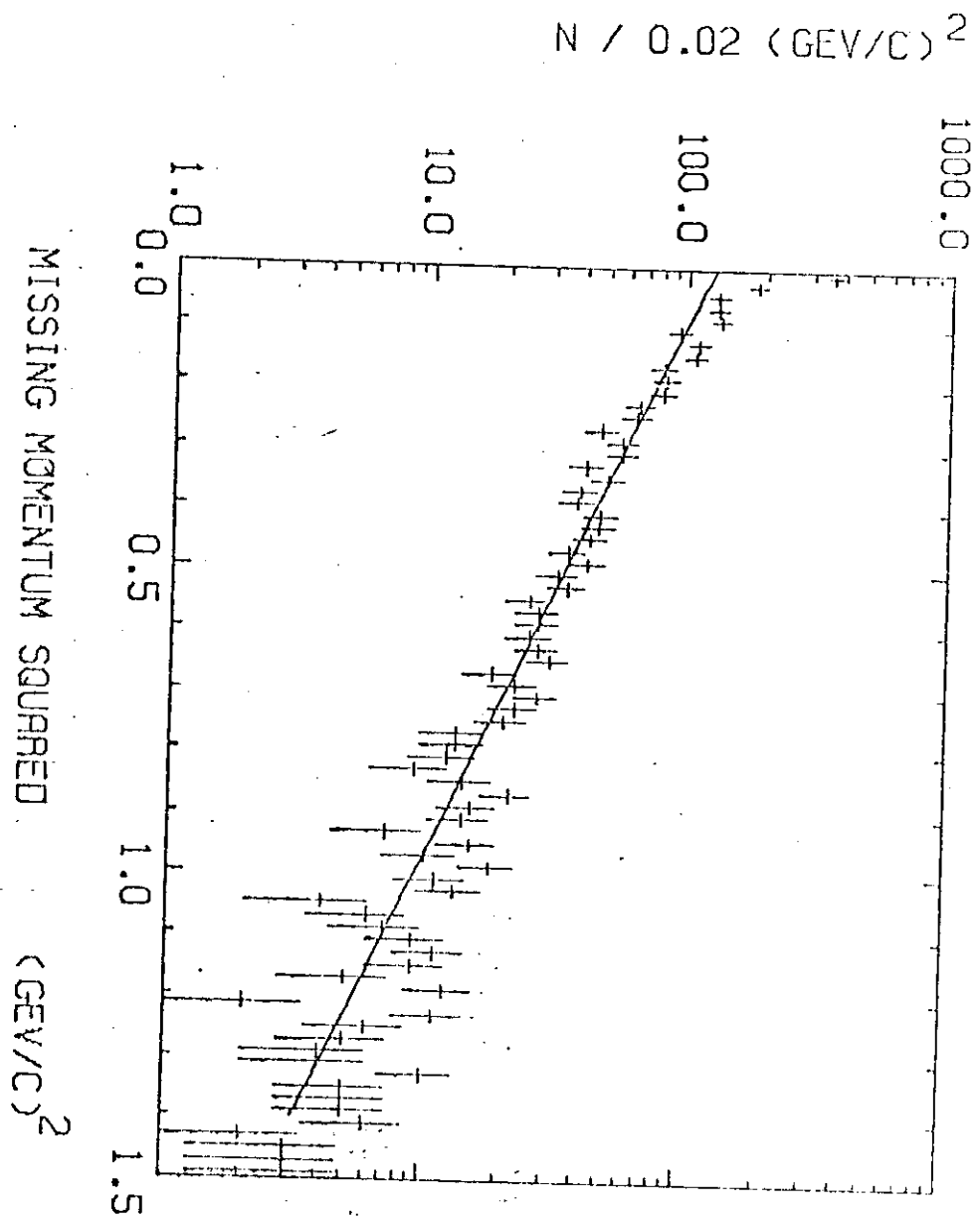


fig 15d

II The 4.0 - 4.4 GeV region

1. Performance of DORIS :

every 4. bunch only filled

$$\left. \begin{array}{l} I \approx 150 \text{ mA / beam} \\ \tau \approx 5 - 8 \text{ h} \\ vac \approx (5 - 8) \cdot 10^{-9} \end{array} \right\} \approx$$

$$L \approx 10^{30} \text{ cm}^{-2} \text{ sec}^{-1}$$

$$L_{sp} \approx 5 \cdot 10^{31} \text{ cm}^{-2} \text{ sec}^{-1} \text{ Amp}^{-2}$$

$$\int L dt \approx 30 - 50 \text{ nb}^{-1} / \text{day}$$

total of $\sim 1500 \text{ nb}^{-1}$ in the 4 GeV region.

2. Recent results :

DASP : e^{\pm} -hadron - events
(\sim DESY 76/37)

PLUTO : e^{\pm} - K^0 -events
(\sim talk by H. Meyer)